European Commission

JRC VALIDATED METHODS, REFERENCE METHODS AND MEASUREMENTS

The certification of the mass fraction of carbon in cementite grains in a Fe-C matrix: IRMM-471

S. R. J. Saunders, T. Bacquart, J-F. Almagro, A. Braun, P. Busch, O. Couteau, D. D. Gohil, P. Karduck, G. Kerckhove, T. Linsinger, S. Richter, G. Roebben, X. Sauvage, W. G. Sloof, J-F. Thiot, M. Whitwood, T. Wirth

2013

Report EUR 25843 EN

Joint Research Centre

European Commission
Joint Research Centre
Institute for Reference Materials and Measurements

Contact information
Thomas Bacquart
Address: Joint Research Centre, Retieseweg 111, B-2440, Geel, Belgium
E-mail: thomas.bacquart@ec.europa.eu
Tel.: +32 (0)14 571 721
Fax: +32 (0)14 571 548

http://irmm.jrc.ec.europa.eu/
http://www.jrc.ec.europa.eu/

JRC79149

EUR 25843 EN

ISBN 978-92-79-28809-8 (PDF)

ISSN 1831-9424 (online)

doi:10.2787/77197

Luxembourg: Publications Office of the European Union, 2013

Printed in Belgium

The certification of the mass fraction of carbon in cementite grains in a Fe-C matrix: IRMM-471

S. R. J. Saunders[1], T. Bacquart[11], J-F. Almagro[2], A. Braun[11], P. Busch[3], O. Couteau[11], D. D. Gohil[1], P. Karduck[4], G. Kerckhove[11], T. Linsinger[11], S. Richter[5], G. Roebben[11], X. Sauvage[8], W. G. Sloof[6], J-F. Thiot[7], M. Whitwood[9], T. Wirth[10]

[1]National Physical Laboratory, Teddington (UK)
[2]Acerinox S.A., Los Barrios (ES)
[3]Thyssen Krupp Stahl GmbH, Duisburg (DE)
[4]HDZ GbR, Herzogenrath (DE)
[5]RWTH Aachen, Aachen (DE)
[6]Technische Universiteit Delft (TUD), Delft (NL)
[7]SAMx, Gyuancourt (FR)
[8]Centre National de la Recherche Scientifique (UMR 6634), Rouen (FR)
[9]Corus plc, Rotherham (UK)
[10]Bundesanstalt für Materialforschung und -prüfung (BAM), Berlin, (DE)
[11]European Commission, Joint Research Centre,
Institute for Reference Materials and Measurements (IRMM), Geel (BE)

Disclaimer

Certain commercial equipment, instruments, and materials are identified in this paper to specify adequately the experimental procedure. In no case does such identification imply recommendation or endorsement by the European Commission, nor does it imply that the material or equipment is necessarily the best available for the purpose

Summary

This report describes the production and certification of IRMM-471, a reference material certified for the carbon mass fraction of its cementite (Fe_3C) grains. The Fe_3C grains are dispersed within an iron pearlite matrix and present an average grain diameter between 20 µm and 50 µm.

The compound was produced by carburising pure iron under carefully controlled conditions.

Between-points inhomogeneity was quantified and stability during dispatch and storage was assessed. Within-grains inhomogeneity was quantified to determine the minimum sample intake.

The certified value of the carbon mass fraction in the cementite grains was obtained from the thermodynamic evidence that Fe_3C exists as a line compound i.e. it has a single composition defined by its stoichiometry. The presence of single grains of the cementite phase in the iron pearlite matrix was confirmed by X-ray diffraction and by electron diffraction methods: Electron Backscattered Pattern technique (KIKUCHI technique) and micro-X-ray diffraction method (KOSSEL technique).

The certified value of the carbon mass fraction was confirmed by Atom Probe Tomography as an independent method.

Uncertainties of the certified value were calculated in compliance with the Guide to the Expression of Uncertainty in Measurement (GUM) [1] and include uncertainties related to possible inhomogeneity, instability and characterisation.

The material is intended for calibration, quality control and assessment of method performance. As any reference material, it can also be used for control charts or validation studies. The CRM is available in a polypropylene box containing a rod of 5 mm diameter 4 mm to 5 mm length of pearlite matrix with a dispersed phase of cementite (Fe_3C). The minimum amount of sample to be used is a volume of 0.000024 μm^3.

The following values were assigned:

	Mass Fraction	
	Certified value [1)] [g/kg]	Uncertainty [2)] [g/kg]
Carbon mass fraction in cementite grains	66.9	2.7

1) Value based on Fe_3C stoichiometry corresponding with the thermodynamic assessment that Fe_3C exists as a line compound (i.e. it has a single stoichiometric composition) confirmed by 4 accepted sets of data, each set being obtained in a different laboratory and/or with a different method of determination. The certified value and its uncertainty are traceable to the International System of units (SI).

2) The certified uncertainty is the expanded uncertainty with a coverage factor k = 2 corresponding to a level of confidence of about 95 % estimated in accordance with ISO/IEC Guide 98-3, Guide to the Expression of Uncertainty in Measurement (GUM:1995), ISO, 2008.

Table of content

Glossary

AES	Auger electron spectrometry
ANOVA	Analysis of variance
APT	Atom probe tomography
b	Slope in the equation of linear regression $y = a + bx$
BCR®	One of the trademarks of CRMs owned by the European Commission; formerly Community Bureau of Reference
CCD	Charge-coupled device
CI	confidence interval
CRM	Certified reference material
EBSP	Electron backscattered pattern
EC	European Commission
EN	European norm (standard)
EPMA	Electron probe micro analysis
EU	European Union
FEG	Field emission gun
FIB	Focused ion beam
GUM	Guide to the Expression of Uncertainty in Measurements *[ISO/IEC Guide 98-3:2008]*
IRMM	Institute for Reference Materials and Measurements of the JRC
ISO	International Organization for Standardization
JCPDS	Joint Committee on Powder Diffraction Standards
JRC	Joint Research Centre of the European Commission
k	Coverage factor
MS	Mass spectrometry
MS	Mean of squares
n	Number of replicates per unit
N	Number of samples (units) analysed
OPS	Oxide polishing suspension
rel	Index denoting relative figures (uncertainties etc.)
RM	Reference material
RSD	Relative standard deviation
r^2	Coefficient of determination of the linear regression
s	Standard deviation
SEM	Scanning electron microscope

$s_{between}$	Standard deviation between groups as obtained from ANOVA; an additional index "rel" is added as appropriate
SI	International System of Units
SiC	Silicon carbide
T	Temperature
t	Time
t_i	Time point for each replicate
t_{sl}	Proposed shelf life
u	standard uncertainty
U	expanded uncertainty
u_{bb}	Standard uncertainty related to a possible between-unit homogeneity; an additional index "rel" is added as appropriate
u_{char}	Standard uncertainty of the material characterisation; an additional index "rel" is added as appropriate
u_{CRM}	Combined standard uncertainty of the certified value; an additional index "rel" is added as appropriate
U_{CRM}	Expanded uncertainty of the certified value; an additional index "rel" is added as appropriate
u_{Δ}	Combined standard uncertainty of measurement result and certified value
UHV	Ultra high vacuum
u_{lts}	Standard uncertainty of the long-term stability; an additional index "rel" is added as appropriate
u_{sts}	Standard uncertainty of the short-term stability
UV	Ultraviolet
V	Volume
WDXRF	Wavelength-dispersive X-ray fluorescence spectrometry
$\overline{x}$	Arithmetic mean
XRD	X-ray diffraction
$\overline{x_{ref}}$	Arithmetic mean of results of reference samples
α	significance level
Δm	Absolute difference between mean measured value and the certified value
σ^2_W	Total variance
σ^2_{BW}	Population variance of production batch means
σ^2_{SW}	Population variance of specimen means within production batches
σ^2_{PW}	Population variance of point means within specimen

1 Introduction

1.1 Background

Many materials have complex microstructures, the chemical and structural aspects of which crucially determine performance. Thus measurement methods are required to describe these microfeatures accurately. Electron-probe microanalysis (EPMA) is widely used in industry, commercial laboratories and research organisations to determine the chemical composition of areas only a few micrometres in diameter. Although widely used, the standardization of the measurement method is recent and lead by ISO Technical Committee 202/SC 2 which developed several ISO standards for determining carbon content in steel (ISO 16592:2006) [2] or for quantitative point analysis by WDXRF (ISO 22489:2006) [3]. The important issue of light element analysis, especially carbon, was addressed in ISO 16592:2006 guidelines for determining the carbon content of steels using a calibration curve method [2].

The guidelines in ISO 16592:2006 [2] do not address high carbon content steel and only focus on steel with a C mass fraction less than 10 g/kg to 20 g/kg. However, carbon mass fraction analysis is not limited to materials with carbon mass fraction below 20 g/kg. In many materials, particularly steels, corrosion and wear resistant coatings, iron carbides play a major role in determining performance, but light elements (low atomic number) are difficult to analyse by EPMA, and special methods have to be devised. Increasing tightness of specifications requires highly accurate analysis. Because of the importance of the measurement method, many different organisations have developed their own "in house" calibrants.

1.2 Choice of the material

In the extensive studies of Bastin and Heijligers [4] on microprobe analysis of carbon in binary carbides it was established that the cementite phase, Fe_3C, is particularly well suited as a reference material for the analysis of C. This compound is (i) electrically conductive, (ii) is a so called "stoichiometric line compound" (i.e. its composition is well established at carbon mass fraction of 66.9 g/kg) and, (iii) has good long-term stability. Although Fe_3C is thermodynamically metastable, it is known to be sufficiently stable at room temperature. All these reasons favoured the certification of the C content in a cementite phase.

1.3 Design of the project

A feasibility study was carried out to determine the optimal route for production of the desired material. Different carburizing approaches were tested using pack carburization, austenitic and ferritic techniques. These approaches lead to the production of iron carbide grains with grain size less or around 20 µm, which were considered too small for this CRM. The development of gas carburisation was preferred in order to obtain larger cementite grains (~ 50 µm). The optimized process for production of large cementite grains (~50 µm grain size) consists of taking drawn rods of pure iron through successive thermal treatments in CO gas. Having established a satisfactory production route, sufficient specimens were produced for the certification (237 specimens). Their homogeneity was established at the micrometre level using EPMA.

The stability of the material was established according to tests in which specimens and packaging were exposed to extremes of temperature, ultraviolet radiation and humidity expected under “normal” storage conditions. The reference materials produced were checked for homogeneity at the micrometer level.

The certification was based on the established stoichiometry of the compound. The presence of cementite was confirmed by the identification of single grains of a well defined single

phase of cementite (Fe_3C). Additionally, the stoichiometric composition was investigated by direct determination of carbon in the cementite phase by Atom Probe Tomography.

2 Participants

2.1 Project management and evaluation

National Physical Laboratory (NPL), Teddington (UK)

European Commission, Joint Research Centre, Institute for Reference Materials and Measurements (IRMM), Geel (BE)

2.2 Processing

Gemeinschaftslabor für Elektronmikroskopie, RWTH Aachen, Aachen (DE)

HDZ, GbR, Herzogenrath (DE)

2.3 Homogeneity study

Bundesanstalt für Materialforschung und -prüfung (BAM), Berlin (DE)

Corus plc, Rotherham (UK)

Gemeinschaftslabor für Elektronmikroskopie, RWTH Aachen, Aachen (DE)

National Physical Laboratory (NPL), Teddington (UK)

2.4 Stability study

Bundesanstalt für Materialforschung und -prüfung (BAM), Berlin (DE)

Gemeinschaftslabor für Elektronmikroskopie, RWTH Aachen, Aachen (DE)

National Physical Laboratory (NPL), Teddington (UK)

2.5 Characterisation

ACERINOX S.A., Los Barrios (ES)

EKO Stahl GmbH, Eisenhüttenstadt (DE)

European Commission, Joint Research Centre, Institute for Reference Materials and Measurements (IRMM), Geel (BE)

Groupe de Physique des Matériaux, UMR CNRS 6634, Rouen (FR)

HDZ, GbR, Herzogenrath (DE)

Institut für Werkstoffwissenschaften, Technische Universität, Dresden (DE)

National Physical Laboratory (NPL), Teddington (UK)

SAMx, Guyancourt (FR)

Technische Universiteit Delft, (TUD), Delft (NL)

Thyssen Krupp Stahl GmbH, Duisburg (DE)

3 Material processing and process control

The phase diagram of the Fe-C system is well established. It is the basis of steel making and steel processing and thus reliable data exist which were used as a basis for the present work [5-6].

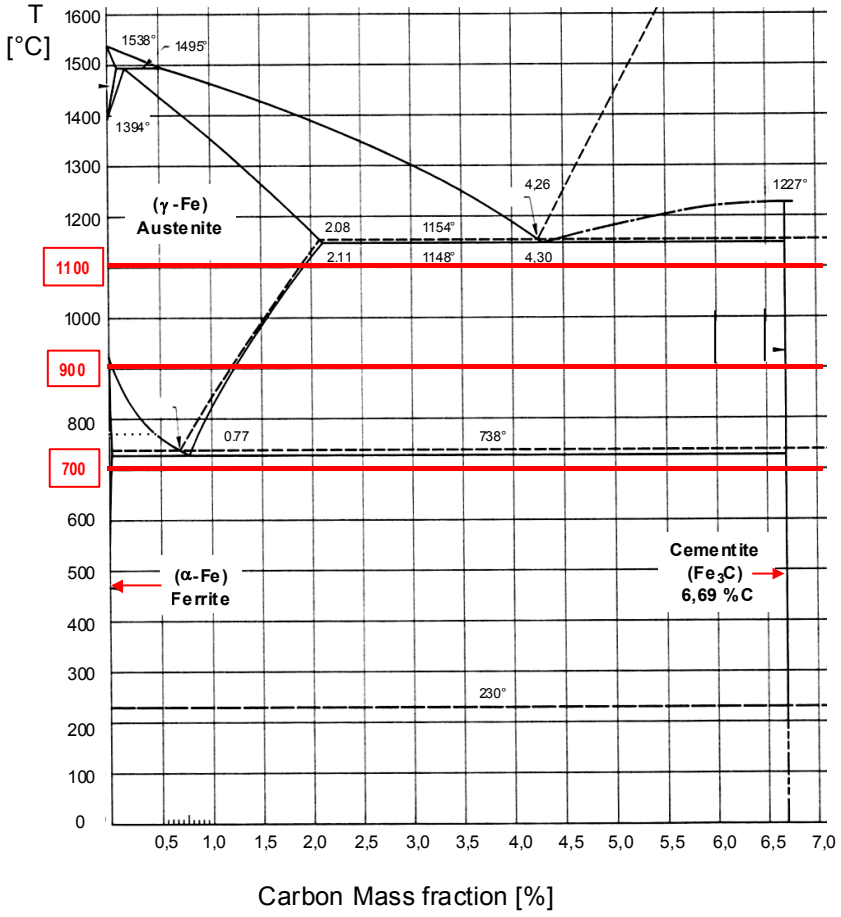

Figure 1: Phase diagram Fe – C (dashed line: the metastable Fe – Fe_3C system). The temperatures of the single carburization steps are marked.

The objective of the present study was to carburize high purity iron over an extended period in a CO-containing atmosphere at high temperatures. It was expected that such a process would produce large precipitates of the carbide embedded in a ferritic or pearlitic matrix. But since the CRM is aimed for application in microbeam analysis it would be sufficient if the Fe_3C-grains were larger than about 30 µm diameter. The interaction volume from which the X-rays emerge after excitation by an electron beam is typically in the range of 5 μm^3 to 10 μm^3 in a Fe-matrix.

Because of complex thermodynamics and kinetics of the iron–carbon–system, preparation of large homogenous cementite (Fe_3C) grains is somewhat empirical. Carburising agent, pureness of the iron, reaction furnace system and importantly reaction temperature and cooling rate are all key parameters in the formation of Fe_3C. All parameters form a complex relationship between nucleation, mass transport and growth rate. The aim of this investigation was to optimize the growth of large, homogeneous Fe_3C grains.

After a feasibility study, the optimized process for production of large cementite (Fe_3C) grains (~50 µm grain size) consists of taking drawn rods of pure iron (Vacofer©) through successive thermal treatments in 99 % CO gas. The metallographic preparation of the rods was realised in order to produce 237 units. Section 3.2.2 details the various steps of metallographic

preparation from the carburized rods to the final specimen (rod of 5 mm diameter by 4 mm to 5 mm length).

3.1 Origin of the starting material

The starting materials were high purity iron rods with > 99.98 % Fe (product reference: Vacofer S1), produced by Vacuumschmelze (Hanau, DE).

3.2 Processing

The processing took place at RWTH Aachen in Aachen (DE). It was divided into two parts:

- Carbide production by carburization of the iron rods under carefully controlled conditions,

- Metallographic preparation of the materials.

3.2.1 Carbide production by carburization

Gas carburization of the iron rods was carried out using 99 % pure CO gas in a horizontal furnace with an alumina reaction tube with a constant temperature zone of 50 mm. The CO gas flow rate was 2 L/h and a wash bottle at the end of the line was used to prevent back diffusion of air into the furnace tube. The specimens were furnace cooled under flowing CO gas. With this furnace, 10 – 12 rods (∅ 5 mm, length 50 mm) could be treated in one run. In order to produce the required 237 units 3 batches were produced in individual runs.

With the gas carburization process, constant conditions could be guaranteed over long periods. During the process, the flow rate and the temperature were controlled by a gas flow-meter and the furnace temperature (± 5 °C) to ensure constant conditions. In addition, the temperature was monitored in the gas flow near the Fe rods using Pt/Rh thermo couple. Soot formation on the inner surface of the Al_2O_3-tube at temperatures above 900 °C would eventually build up and block gas flow. Thus to overcome this problem a four-step heating process was chosen as listed below:

- Recrystallization at 700 °C for 4.5 h;
- Carburization at 900 °C for 180 h;
- Further carburization and cementite grain growth at 1100 °C for 8 h;
- Cementite grain growth by furnace cooling from 1100 °C to 727 °C at 10 °C/h.

Following these steps the carburized rods were ready for further processing.

3.2.2 Metallographic preparation of CRMs

Three main steps were followed in order to prepare the final specimen: cutting the sample into a specimen of suitable dimension, side preparation, and the final cleaning and inspection.

All specimens were prepared in such way that the side of the specimen was flat and it was important to ensure that there was no rounding at the edge of the individual Fe_3C precipitates. Only one of the flat sides of the specimen was prepared through 3 steps: grounding, lapping and polishing. After each preparation step the specimens were thoroughly cleaned and dried.

a) Cutting

The rods were cut into 5 mm long pieces with a thin blade (less than 1 mm) diamond saw. Ethanol was used as a lubricant. The top of each rod was defined as the end where the rod was labelled with a letter. Starting at the bottom of each rod, the first piece was denoted as specimen 00. This specimen was not used. The next specimen was denoted as 01 and the following as 02 and so on. The last part of the rod (with the label) was also not used. Each

piece represents an IRMM-471 specimen. In total, approximately 8 specimens were produced from each rod.

b) Side preparation

One side of the specimen was successively ground, lapped and polished. After each preparation step the specimens were cleaned thoroughly and dried. A special tool was developed for metallographic preparation to hold and machine the specimens (see Figure 2). A total of six specimens could be mounted in this tool. The specimens were put into the holes such that the side was at the same level as the side of the tool, and were fixed in the tool by a screw.

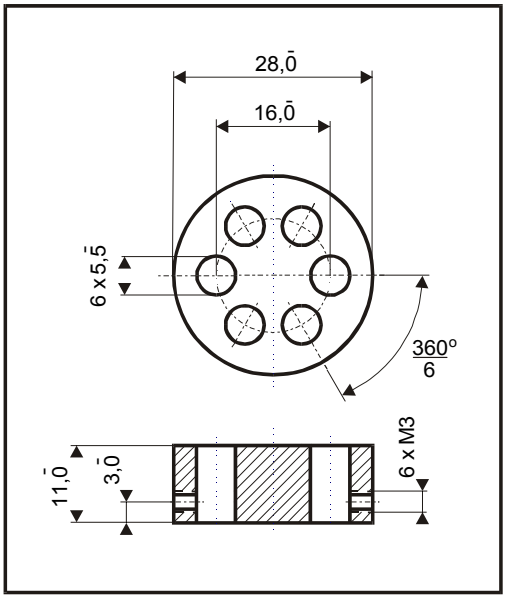

Figure 2: Specimen holder for metallographic preparation.

First, the specimens were ground with silicon carbide (SiC) paper flushed with water. Usually, it sufficed to start with 320 SiC paper. Then, 400 and 600 SiC emery papers were applied successively. After the grinding process, the tool with the mounted specimens was thoroughly cleaned ultrasonically for 5 minutes using ethanol. Next, the assembly was dried with compressed pure nitrogen gas.

To provide a flat side on each specimen, i.e. no curvature particularly near the edge of the specimens, the specimens were lapped using a 9 µm diamond suspension. After the lapping process the tool with the mounted specimens was thoroughly cleaned ultrasonically for 5 minutes using ethanol. Next, the assembly was dried with compressed pure nitrogen gas. Special attention was paid to clean the spaces between the holes of the tool and the specimens to ensure complete removal of grinding debris.

After the lapping process, the specimens were polished in a sequence of steps. An automatic polishing machine was used to ensure flatness of the specimens. First, the specimens were polished with 3 µm diamond on a hard cloth using an oil-based fluid as a lubricant. Then, the samples were polished with 1 µm diamond suspension applied also on a hard cloth and using an oil-based fluid as a lubricant. Finally, the specimens were polished for a maximum of 30 seconds using OPS on an appropriate cloth and demineralised water as a lubricant. After each polishing step, the tool with the mounted specimens was cleaned thoroughly using the same cleaning procedure as after lapping.

c) Final cleaning, storage and inspection

After completion of the metallographic preparation, the Fe_3C specimens were removed from the preparation tool, cleaned thoroughly, dried (same cleaning procedure as after lapping) and stored indivudually in a polypropylene box.

Each specimen was denoted by a code: Fe_3C X ##; where X = A, B, C, D, E, F, G, H, I or J corresponding with the label on the carburized rod, and where ## is a two digit number corresponding with the number of the specimen cut from the rod. For example, Fe_3C B 04 is the specimen with number 04 cut from carburized iron rod B. IRMM maintains traceability from IRMM-471 unit number to specimen position in rod, rod number and batch number.

At the end of the processing, each specimen was inspected using an optical microscope. The polished side of the specimen must be free of severe scratches or flaws. Some minor defects (graphite inclusions / pores) were present on some specimens. These minor defect areas (ranging from few micrometres to few hundred micrometres as shown in Figure 3) should not be sampled for analysis. Nonetheless, these minor defects do not affect the quality of the specimen for the use as a calibrant.

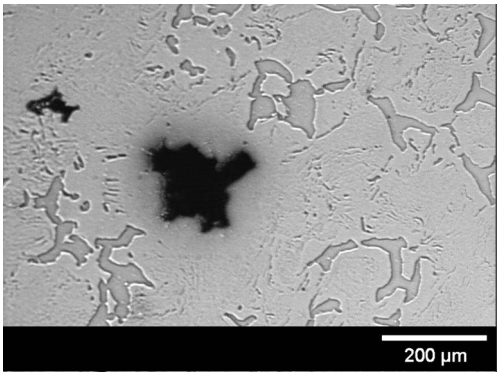

Figure 3: Optical micrograph of defect on a reference specimen.

4 Homogeneity

A key requirement for any reference material is the equivalence between the various units. In this respect, it is relevant whether the variation between units is significant compared to the uncertainty of the certified value. In contrast to that it is not relevant if this variation between units is significant compared to the analytical variation. Consequently, ISO Guide 34 [7] requires RM producers to quantify the between unit variation. This aspect is covered in between-unit homogeneity studies.

In the special case of the certification of cementite (Fe_3C) grains in an iron/pearlite matrix, the certified material is composed of Fe_3C grains dispersed in the specimen and using EPMA, it is possible to spatially resolve and analyse carbon within a single grain of Fe_3C.

The definition of homogeneity will follow the definition given in the standard ISO 14595:2003 [8], which defines the different contributions to homogeneity as the uncertainties in the measurements from specimen to specimen, from micrometre to micrometre within each specimen, and from the test procedure itself. In the present certified material, the uncertainty from micrometre to micrometre will be replaced by the uncertainty from point to point within specimen which covers uncertainty from grain to grain within specimen and uncertainty from point to point within Fe_3C grain (point is the analysed area by EPMA).

The within-grain inhomogeneity of the cementite precipitate in a specimen does not influence the uncertainty of the certified value when the minimum sample intake (point dimension) is respected, but determines the minimum size of a sample volume that is representative for the whole grain. Quantification of within-grain inhomogeneity is therefore necessary to determine the minimum sample intake.

In the evaluation of homogeneity, the final uncertainty will include the homogeneity between specimens, homogeneity between batches and the micro homogeneity (variation between points within specimens).

4.1 Between-point homogeneity

The between-point homogeneity was evaluated to ensure that the certified values of the CRM are valid for all 237 specimens of the material, within the stated uncertainty. The between point homogeneity scheme allowed the study of within-specimen, between-specimen and between-batch variation.

For the between-point homogeneity test, 9 specimens were selected from across the whole production. For this, the production was divided into 3 groups (corresponding to the three production batches) and two rods were selected from each group. From the two rods selected, three specimens in total were selected randomly (1 specimen from 1 rod, 2 specimens from the other rod). From each specimen, 104 measuring points were analysed from 20 different Fe_3C grains by EPMA. The measurements were performed under reproducibility conditions in two laboratories (BAM and GFE). The same measurements were made on an "in house" Fe_3C calibrant. Fe-Kα radiation was measured simultaneously with the measurement of the C-Kα radiation. The measurement setup is detailed in Annex A.

For an additional evaluation of the trend within a single carburized rod, 3 rods were taken from the feasibility study. The rods were produced using the same process as rods used to make the CRM specimens. The analytical procedure was similar for the homogeneity study on CRM specimens. On each rod, three specimens were selected to evaluate as follows: one from each extremity of the rod and one from the centre.

Regression analyses were performed to evaluate potential trends in the processing sequence and in the rod position (both ends and the middle). No regression lines in the processing sequence and in the rod position were statistically different from 0 at 99 % confidence level. The results are shown as graphics in Annex A.

Evaluation by ANOVA requires specimen means which follow at least a unimodal distribution and results for each specimen that follow unimodal distributions with approximately the same standard deviations. Distribution of the specimen averages was visually tested using histograms and normal probability plots. Minor deviations from unimodality of the individual values do not affect the estimate of between-unit standard deviations. The results of all statistical evaluations are given in Table 1.

Table 1: Results of the statistical evaluation of homogeneity studies data at 99 % confidence level.

Method/Measurand	Trends		Outliers	Distribution
	Rod position	Processing sequence	Specimen means	Specimen means
Electron Probe MicroAnalysis	no	no	none	unimodal

All data were analysed using a procedure detailed in Annex F in three stages: (a) pre-processing of the data into a form suitable for a standard Analysis of Variances (ANOVA), (b) performing the ANOVA analysis and (c) post processing to provide the measurement result. The ANOVA analysis was carried out using a specially designed and tested EXCEL spreadsheet by NPL. The analysis distinguishes uncertainty in the data at four levels - replicates on a given point, point to point within a single specimen, specimen to specimen and finally production batch to production batch. The design of the study allows the uncertainty from each level to be compared to determine the significance of the uncertainty using the F-test. The statistical analysis is given in Annex F. Comparison of the variances shows that between batch and between specimen effects are not significantly larger than the between points effect (F-tests performed at the confidence interval of 95 %). The results can be pooled to give a single standard deviation u_{bb} expressed in g/kg for all 9*104 measurements.

Table 2: Results of statistical analysis of C-Kα of Fe_3C specimens from three production batches, three specimens each batch; mass fraction of carbon: 6.69 g/100 g; mass fraction of iron: 93.31 g/100 g.

Statistical analysis of the C-Kα measurement	**Symbol**	**Results based on raw data [(g/100 g)^2]**
Variance of production batches means	σ^2_{BW}	-0.0026 (Mean Squared values between Specimens > Mean Squared values between Batches)
Variance of specimen means within production batches	σ^2_{SW}	0.0092
Variance of point means within specimen	σ^2_{PW}	0.0105

The total variance determined by the statistical analysis of the C-Kα measurement was used as a good estimate of u_{bb}^2. Relative between unit uncertainty was calculated as follow:

$$u_{bb,rel} = \frac{u_{bb}}{certifiedvalue} \times 100 \qquad \textbf{Equation 1}$$

Table 3: Results of homogeneity study and calculation of between unit uncertainty.

Homogeneity study	**Results**	**Unit**
Total variance (σ^2_W)	0.0170	[(g/100 g)^2]
Between unit uncertainty $u_{bb} = \sqrt{\sigma^2_W}$	0.130	[g/100 g]
Between unit uncertainty (u_{bb})	1.30	[g/kg]
Relative Between unit uncertainty	1.95	[%]

The expected variation in composition is very small (because Fe_3C is a line compound). Therefore, all observed scatter and the associated variances are probably artefacts of the testing procedure and can not be used to draw any conclusions about real inhomogeneity. Nevertheless, u_{bb} gives the best available estimation of the variation within-specimen, between-specimen and between-batch, even if it includes variation due to the test procedure (EPMA).

4.2 Minimum sample intake (within a cementite grain)

The within-grain homogeneity is closely correlated to the minimum sample intake. Due to the intrinsic inhomogeneity (local lattice defects such as interstitial, substitutional atoms or vacancies), local area analysed (by micro-analysis technique) in cementite (Fe_3C) grains of a material may not contain the same amount of analyte. The minimum sample intake is the minimum amount or volume of sample that is representative for the whole grain and the whole specimen and thus can be used in an analysis. Sample sizes equal or above the minimum sample intake guarantee the certified value within its stated uncertainty.

The minimum sample intake was determined from the results of the characterisation study, using the information obtained by Atom Probe Tomography. The smallest sample intake that

still yielded technically accepted results with acceptable precision (RSD better than 2 %) was taken as minimum sample intake. Using the data from Annex D and considering an average atomic volume of 0.012 nm^3 in Fe_3C, the minimum sample intake is derived from APT analysis, which uses a volume of 0.000024 μm^3.

5 Stability

Thermodynamic predictions indicate that Fe_3C is stable at room temperature when stored under dry conditions [4-6]. The slow cooling step in the thermal process (cooling rate 10° C/h) gives more assurance on the stability of the material. For these reasons, the material is assumed to be stable.

Nevertheless stability testing is performed to confirm this assumption under the chosen conditions for storage (long-term stability) as well as conditions for dispatch to the customers (short-term stability). During transport, especially in summer time, temperatures up to 60 °C could be reached and stability against these conditions must be demonstrated if transport at ambient temperature is used.

Time, humidity, temperature and radiation were regarded as the most relevant influences on stability of the materials. Even if the influence of ultraviolet or visible radiation was minimised by the choice of the containment, the influences of time, UV radiation, humidity and temperature were nevertheless investigated.

The stability studies were carried out using a classical stability design. In that approach, samples are stored for a certain time in different conditions (temperature, humidity, UV radiation) and the samples are analysed at the end of the respective time. The analyses were carried out under reproducibility conditions. To compare the results from different times and conditions, all analysis were compared to the same reference sample stored at reference temperature and in normal conditions.

5.1 Short-term stability study

For the short-term stability study, the influence of temperature, humidity and UV radiation were checked particularly with regard to the packaging of the specimens. The specimens were stored in a hard plastic case that is held within an outer plastic box containing silica gel. The following tests were carried out with specimens stored in the packaging system described above. Before starting the testing procedures, all the specimens were analysed by optical microscopy and AES.

A) Temperature stability: Two samples were selected using a random stratified sampling scheme. One specimen and its box were stored in an oven at +110 °C and the other in a cold chamber at –50 °C for one week followed by surface investigation by optical microscopy and AES. After analysis the tests were repeated on the way that the heated specimen was cooled and the cooled specimen was heated. All specimens were again analysed by optical microscopy and AES after finishing these second test series. Then, they were subjected to the final stage of polishing (ie a maximum of 30 seconds using OPS on an appropriate cloth using demineralized water as a lubricant) and the compositions were checked on 50 points of the specimen by EPMA. The measurements were performed under reproducibility conditions.

B) Humidity and UV radiation stability: Samples were stored at two different conditions: 23 °C 12 % humidity for 12 weeks and 40 °C, 50 % humidity for 12 weeks. During this period the specimens were located behind a glass window and were exposed to UV radiation of 50 W/m². One sample per condition was selected using a random stratified sampling scheme. The samples were measured by optical microscopy, EPMA and AES on 50 points of the specimen. The measurements were performed under reproducibility conditions.

The obtained data from test A and test B were evaluated individually for each temperature.

Results of A) Temperature stability:

Figure 4 shows Fe_3C specimens in the as-received condition and Figure 5 after the heating and cooling tests. The surface of Fe_3C specimen does not show significant changes. The carbides were covered by an oxide layer of a thickness of a few nanometres as demonstrated by the AES depth profile (Figure 6).

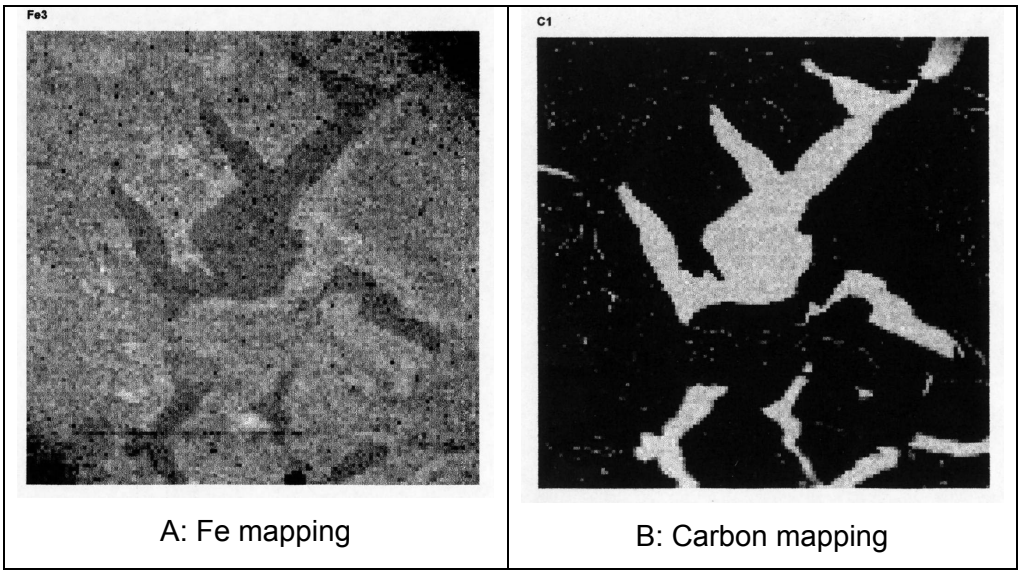

Figure 4: AES results of Fe_3C specimen in the as-received condition. Analysis parameters: windows size: 400 µm, magnification x317, resolution 128 pixels, time per step: 10 milliseconds, beam voltage: 3000 V, beam current: 0.358 µA. For Fe, peak: 700 eV, background: 720 eV, multiplier: 1100 V. For carbon: peak: 270 eV, background E1: 280 eV, multiplier: 1135 V.

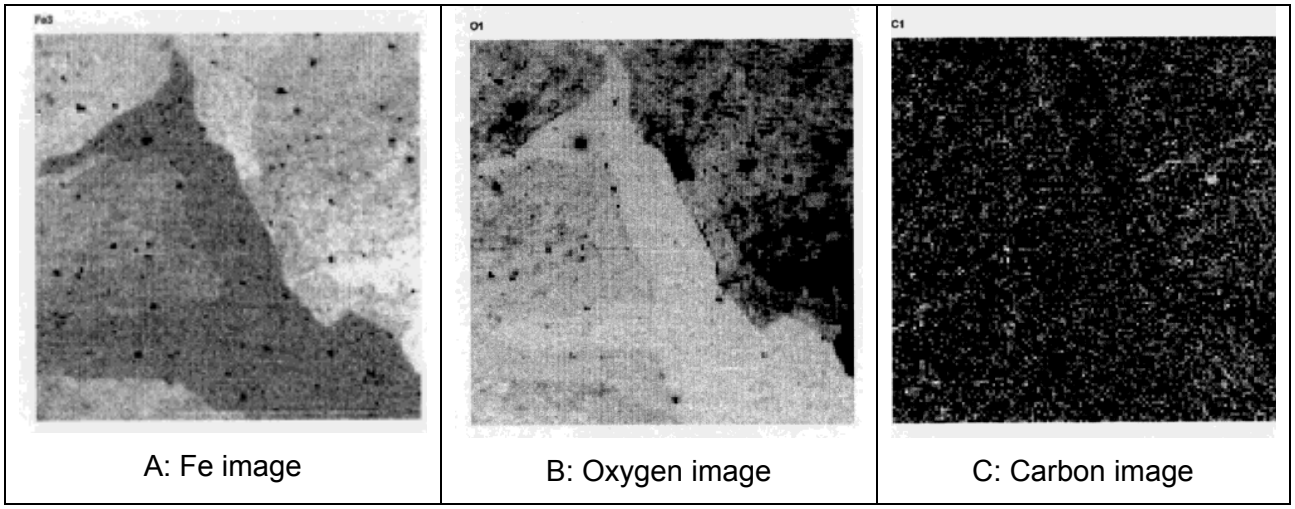

Figure 5: AES results determined on the surface of a heated and cooled Fe_3C specimen. Analysis parameters: windows size: 200µm, magnification x635, resolution 128 pixels, time per step: 10 milliseconds, beam voltage: 3000 V, beam current: 0.358uA. For Fe, peak: 750 eV, background: 720 eV, multiplier: 1100 V. For oxygen: peak: 510 eV, background E1: 535 eV, multiplier: 1105 V. For carbon: peak: 269 eV, background E1: 260 eV, background E2: 255 eV, multiplier: 1135 V.

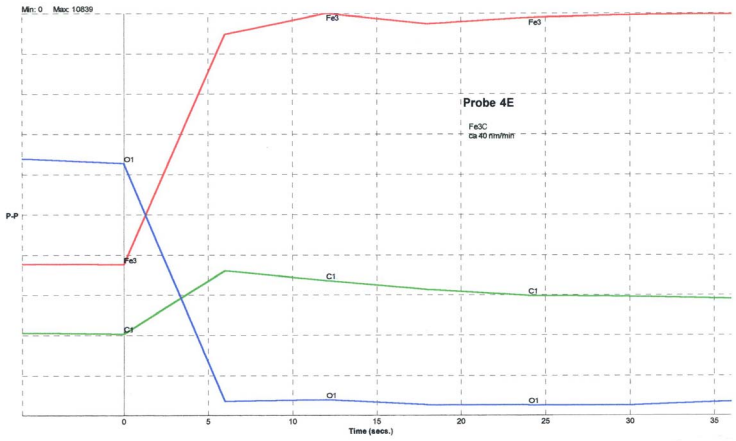

Figure 6: AES depth profile of the surface coverage layer grown on a Fe_3C grain during heating and cooling of the specimen inside the boxes. Blue line annoted O1 is oxygen, green line annoted C1 is carbon, red line annoted Fe3 is iron. Sputter time: 0.6 min; sputtering rate: 40 nm/min; beam: 5000 V.

Results of B) Humidity and UV radiation stability:

After finishing humidity and UV radiation stability tests, all specimens were analysed by optical microscopy and AES. The surfaces of Fe_3C specimens did not show significant changes (e.g. grain size, phase change, inclusions, oxidation). The carbide specimens were covered by an oxide layer of a thickness of a few nanometres (Figure 6), which could be removed easily during the standard re-preparation procedure (see section 9).

EPMA results for short-term stability studies

The obtained results of the different short-term stability conditions were compared with the reference sample stored under normal conditions. The data were plotted against storage time and regression lines of carbon mass fraction versus time were calculated. The slope of the regression lines was tested for statistical significance (loss/increase due to transport conditions). For carbon, the slope of the regression lines was not significantly different from 0 (on 99 % confidence level) for the different conditions applied (A: temperature, B: humidity and UV radiations). Thus, it has been concluded that all Fe_3C specimens were stable under the temperature, humidity and UV conditions applied if the standard re-preparation procedure described in the instruction for use (see Section 9) were applied.

5.2 Long-term stability study

For the long-term stability study, samples were stored at 18 °C for 0, 3, 6, 12 and 120 months. A minimum of one specimen per storage time (2 specimens for 12 months storage time and 3 specimens for 120 months) was selected using a random sampling scheme.

Before starting the testing procedures all specimens were analysed by optical microscopy and AES. After three months storage within the boxes in the laboratory at room temperature, the specimens were analysed again by optical microscopy and AES. No significant changes of the specimen surface (e.g. grain size, phase, inclusions, oxidation) were observed between 0 and 3 months.

Before analysis, all specimens were subjected to the final stage of polishing (i.e. a maximum of 30 seconds using OPS on an appropriate cloth using demineralized water as a lubricant) or to the normal sample preparation for atom probe tomography. For each specimen stored at 18 °C for 0, 3, 6, 12 months, 50 points were measured by EPMA and AES. The measurements were performed under reproducibility conditions (all the analytical series were normalised to the same iron carbide calibrant analysed in each analytical series). For each

specimen stored at 18 °C for 120 months, 2 – 3 analysis were performed by atom probe tomography.

The data were plotted against storage time and regression lines of carbon counts versus time were calculated. The slope of the regression lines was then tested for statistical significance (loss/increase due to storage conditions). For carbon, the slope of the regression lines was not significantly different from 0 (on 99 % confidence level) at 18 °C for 10 years (120 months). The material can therefore be stored at 18 °C ± 5 °C.

The graph of the results is shown in Annex C. The results for the Fe_3C specimens are summarized in Annex C.

5.3 Estimation of uncertainties

Due to the intrinsic variation of measurement results no study can rule out degradation of materials completely, even in the absence of statistically significant trends. It is therefore necessary to quantify the potential degradation that could be hidden by the method repeatability, i.e. to estimate the uncertainty of stability. This means, even under ideal conditions, the outcome of a stability study can only be "degradation is 0 ± x % per time".

Uncertainties of stability during dispatch and storage were estimated as described in [9] for each analyte. As the uncertainty of the linear regression slope is superior to the value of the slope, the uncertainty of the linear regression can be approximated to the standard deviation of carbon mass fraction mean of data points.

In the case of the short term stability study, the uncertainty of the linear regression between the two points was carried out on a conservative way using the following calculation:

$$S_{y.x} = \sqrt{\sum (s_i^{\,2} / n_i)} \qquad \textbf{Equation 2}$$

s_i standard deviation of the mean of specimen i

n_i number of analysis for specimen i

The uncertainty contribution (u_{lts}) is then calculated as the product of the chosen shelf life and the uncertainty of the regression lines as

$$u_{lts} = \frac{S_{y.x}}{\sqrt{\sum (x_i - \bar{x})^2}} \cdot t_{sl} \qquad \textbf{Equation 3}$$

x_i: time point for specimen i

$\bar{x}$: time points of the study of each replicate

t_{sl}: proposed shelf life (60 months at 18 ºC in this case)

The following uncertainties were estimated:

- $u_{sts,rel}$, the uncertainty of degradation during dispatch. This was estimated from the temperature studies (-50 °C / +110 °C) for a time of 0.25 months (1 week). The uncertainty therefore describes the possible change during a dispatch at extreme temperatures lasting for one week.
- $u_{lts,rel}$, the stability during storage. This uncertainty contribution was estimated from the 18 °C studies. The uncertainty contribution therefore describes the possible degradation after 60 months at 18 °C.

The results of these evaluations are summarised in Table 4 and Table 5.

Table 4: Relative uncertainties of stability during dispatch. $u_{sts,rel}$ was calculated for temperature (-50 °C / +110 °C); 50 % humidity and UV radiation of 50 W/m²; 12 % humidity and UV radiation of 50 W/m² and 1 week.

Short Term Stability test – Relative uncertainty	Results [%]
$u_{sts,rel}$ Temperature stability (-50 °C / +110 °C)	0.18
$u_{sts,rel}$ Humidity and UV radiation stability (50 % humidity and UV radiation of 50 W/m²)	0.03
$u_{sts,rel}$ Humidity and UV radiation stability (12 % humidity and UV radiation of 50 W/m²)	0.03

Table 5: Uncertainties of stability during storage. $u_{lts,rel}$ was calculated for a storage temperature of 18 °C and 5 years.

Long Term Stability test – Relative uncertainty	Results [%]
$u_{lts,rel}$ for 60 months at 18 °C	0.31

The uncertainty of stability during dispatch is negligible even at +110 °C and -50 °C or in humid conditions (40 % humidity) and under UV radiation of 50 W/m². Thus, it has been concluded that all Fe_3C specimens were stable in the temperature, humidity and UV conditions applied if the standard re-preparation procedure described in the instruction for use (see Section 9) is applied.

Therefore the material can be transported at ambient conditions without special precautions. Before using the CRM specimen, it is mandatory to polish the CRM specimen in order to eliminate the oxide layer that may have appeared. The protocol to prepare the specimen is defined in the instruction for use (see Section 9).

At ambient temperature and according to the Fe-C phase diagram, cementite is meta-stable. Transformation of Fe_3C into graphite (more stable than cementite) may occur at high temperature and after a long time. Transformation of Fe_3C into graphite during the shelf-life of the certified reference test pieces may happen but slowly.

Given the large sample-to-sample inhomogeneity, the ageing effects are undetectable when testing limited numbers of samples, and the uncertainty contribution from instability is considered to be insignificant.

The long term stability study confirms the basic assumption that the Fe_3C phase in the specimens is stable at room temperature. The results of the long term stability show no significant degradation of the material at 18 °C during 10 years (confidence level of 99 %).

Even if the uncertainty contribution from instability is considered to be insignificant, a shelf-life has to be assigned to the material. Following the evaluation of the long term stability study, a u_{lts} can be derived from the standard deviation of the carbon analysis at each time point. For a shelf life of 5 years the uncertainty of instability ($u_{lts,rel}$ = 0.32 %) is negligible compare to the uncertainty contribution from homogeneity ($u_{bb,\ rel}$ = 1.96 %).

Until further notice, it is decided to specify a limited shelf-life. A period of 5 years is chosen. This validity may be extended as further evidence of stability becomes available.

After the certification campaign, the material will be subjected to IRMM's regular stability monitoring programme to control its further stability.

6 Characterisation

The determination of the certified property value is based on the thermodynamically and crystallographically supported general observation that cementite is a line compound and thus has a well defined composition: Fe_3C. Therefore, the assigned value is directly derived from the Fe_3C stoichiometry: carbon atoms in Fe_3C represent 0.25 of the total atom fraction and the carbon mass fraction equals 66.9 g/kg in the Fe_3C compound. The confirmation of this general observation for the Fe_3C phase in samples of IRMM-471 is described in the characterisation chapter and is based on two points:

i) Confirmation of the presence of a single phase of cementite in the ferrite matrix of IRMM-471 by single phase identification:

Phase identification was carried out using three methods: (1) conventional XRD in which the whole specimen was analysed, (2) higher spatial resolution work in which it was possible to analyse the individual cementite precipitates by X-ray and electron diffraction methods, and (3) Kossel and Kikuchi techniques, respectively [10,11]. The results are evaluated to confirm that the Fe_3C phase has the structure of the crystal lattice that matches the Fe_3C stoichiometry.

ii) Confirmation of the assigned property (carbon mass fraction in cementite grains) by direct measurements of the assigned property by an independent method:

Even if Fe_3C is a line compound as indicated in the Fe-C phase diagram, it is possible that deviations from the Fe_3C stoichiometry occur, for example due to interstitial or substitutional point defects or vacancies in the Fe_3C lattice. To demonstrate absence of bias or gross errors atom probe tomography, a direct and independent method to measure the carbon mass fraction was used (Section 6.2).

6.1 Confirmation by cementite phase identification

In order to determine the assigned property on the basis of thermodynamic proof, it is mandatory to identify cementite as a single phase. To confirm and clearly identify the single phase of cementite in single grains included in the pearlite/iron matrix, different techniques were used in order to probe the sample at different scale:

- Phase identification macro-analysis: determination of the phases present in the specimen by X-ray diffraction.
- Phase identification micro-analysis achieved the identification of cementite crystals in the CRM specimens by non-spectroscopic methods (KIKUCHI technique and KOSSEL technique). The reflection KIKUCHI technique, also known as electron backscattered pattern – EBSP, is an electron diffraction method which provides a sensitive fingerprint for the identification of phases. Each KIKUCHI pattern is characteristic for the particular crystal. The KOSSEL technique is a micro-X-ray diffraction method, in which the X-ray source is generated in the specimen (crystal) itself. The basic requirement is that the micro-volume under investigation must be a single crystal. Identification of phases by this technique is more sensitive and also more reliable than with the reflection-KIKUCHI technique because the diffraction pattern obtained by the KOSSEL technique is an individual fingerprint of the structure and orientation of each single crystal analysed.

6.1.1 Phase identification macro-analysis: conventional XRD

An IRMM-471 specimen was scanned by X-ray diffraction (the measurement setup is detailed in Annex D). After removal of background and $K\alpha_2$ contributions from the raw data, a comparison between the experimental results and pure compounds X-rays diffraction patterns from international database (Joint Committee on Powder Diffraction Standards database: JCPDS) was carried out. Comparison of the standard X-ray diffraction patterns for Fe and C containing phases showed that Fe (bcc, JCPDS file: 06-0696 [12]) and Fe_3C (Cohenite a synthetic iron carbide cementite, JCPDS file: 35-0772 [13]) were present in the specimen. The X-ray diffraction pattern for the Cohenite phase (impurities: Al 0.3 g/kg, Si and Zn 0.1 g/kg, Mg and Ni 0.01 g/kg, Ca, Cu and Ti < 0.01 g/kg) was the pattern who matched the better the IRMM-471 X-ray diffractions spectrum. The X-ray patterns along with the stick patterns for Fe (bcc) and Cohenite (Fe_3C) are shown in Figures 7 and 8, respectively.

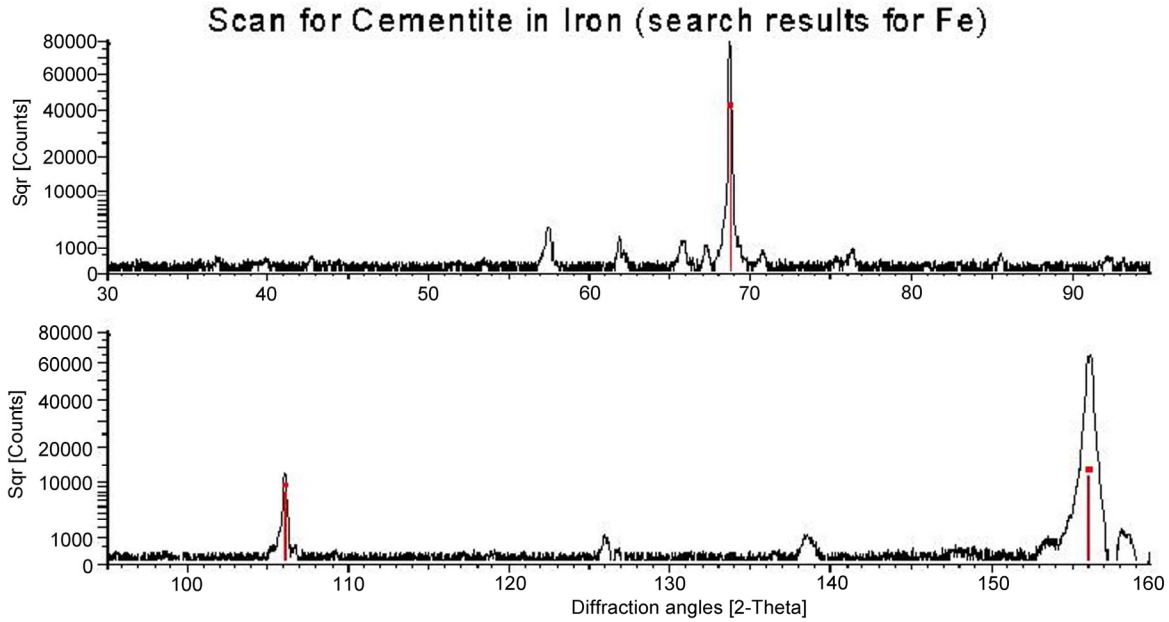

Figure 7: Diffractogram of Fe_3C in Fe matrix recorded with Cr-Kα radiation. Red lines correspond with the HKL-reflections of Fe (bcc) according to JCPDS file 06-0696.

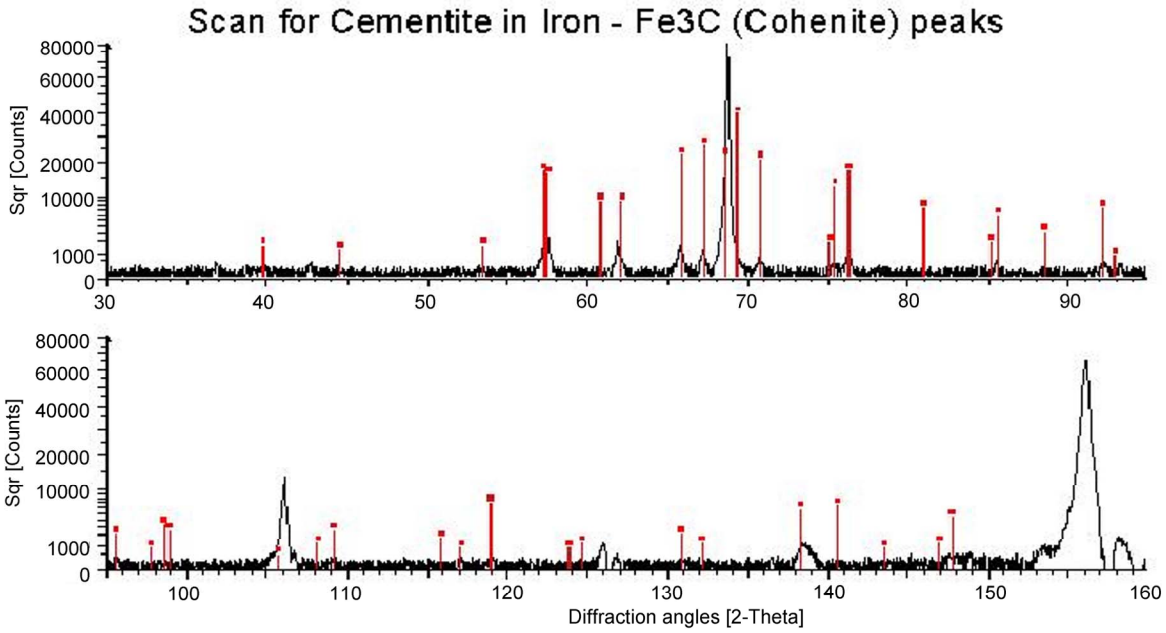

Figure 8: Diffractogram of Fe_3C in Fe matrix recorded with Cr-Kα radiation. Lines correspond with the HKL-reflections of Fe_3C (Cohenite) according to JCPDS file 35-0772.

6.1.2 Phase identification micro-analysis: electron backscattered pattern (reflection Kikuchi technique) and micro-X-ray diffraction method (KOSSEL technique)

Before any micro-analysis, clear identification of the cementite phase in the specimen was done by optical microscopy. Micrographs of suitable areas were recorded. Two different phases could be distinguished in the Fe-matrix: pearlite and cementite. The large Fe_3C-grains had diameters between 20 µm and 50 µm. Thus, the size of the grains was sufficient for examination by micro-diffraction techniques.

For the interpretation of a diffraction pattern the exact knowledge of the crystal structure is required. The crystal structure of Fe_3C detailed by Meinhardt et al. [14] was used to interpret the diffraction patterns.

6.1.2.1 Investigation by the Reflection KIKUCHI technique

The reflection KIKUCHI technique, also known as electron backscattered pattern – EBSP, is an electron diffraction method, which is applied in a scanning electron microscope (SEM). A highly focussed electron beam of defined energy impinges on a tilted specimen at a defined position (Fe_3C-grain). The electrons, which are scattered quasi elastically near the surface, up to depth of a few 10 nm, are diffracted by the lattice planes of the material (Bloch waves). This occurs because those electrons that are scattered in the forward direction posses a cone-like angle distribution and suffer nearly no energy losses. Thus, their wavelength, λ, can be calculated by $\lambda = 1.229nm / \sqrt{E / eV}$. Because of the very small λ of electron waves the opening angle of the diffraction cones is close to 90°. The symmetry planes of the cones are the corresponding families of lattice planes.

The resulting diffraction cones, produced by electron backscattering and diffracted in this way, are projected on to a fluorescing screen and recorded by a CCD-camera. The resulting diffraction pattern contains information about the crystal symmetry and orientation. The pattern is fed into an image processing system and can be evaluated in about a tenth of a second. Thus, by this technique the crystal structure and crystallographic orientation of the excitation volume (< 100 nm when using a field emission gun (FEG)) can be determined. By scanning the beam digitally across the specimen surface so called orientation distribution maps can be recorded.

Each KIKUCHI pattern is characteristic for the particular crystal. KIKUCHI patterns are very sensitive to differing lattice parameters and thus, they provide a sensitive fingerprint technique for the identification of phases [11].

Since in the specimen of interest it is expected that there will be more than one phase with clear differences in crystal structure, it can be assumed that these phases can be distinguished by the reflection Kikuchi technique. In this case the diffraction pattern was expected to be either ferrite (α-Fe) or cementite Fe_3C (Figure 9).

Figure 10 is a secondary electron image of a large homogeneous grain of cementite surrounded by a pearlitic matrix and shows the same structure in a false-colour image. The colour red represents areas in the image that have a diffraction pattern corresponding to the cementite structure. The black pixels in this image could not be attributed clearly to one of the two possible phases. The Figure shows a pole figure with a sharp texture, i.e. only a few orientations are present. Finally, it shows that the large cementite grain is a single crystal that may contain small angle boundaries.

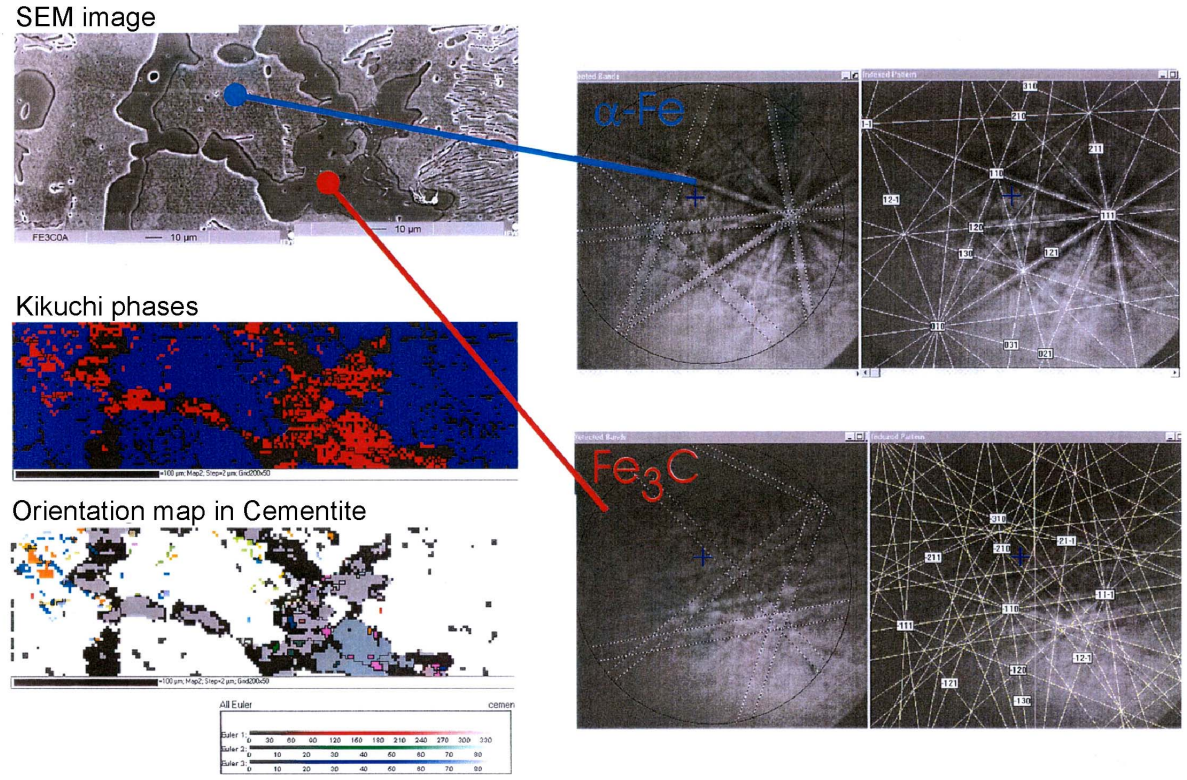

Figure 9: Scanning electron micrograph of the cementite/iron specimen and the corresponding Kikuchi diffraction pattern together with a phase and orientation map for the cementite phase. Red color indicates cementite diffraction pattern; black color indicates undefined diffraction pattern; blue colour indicates iron diffraction pattern.

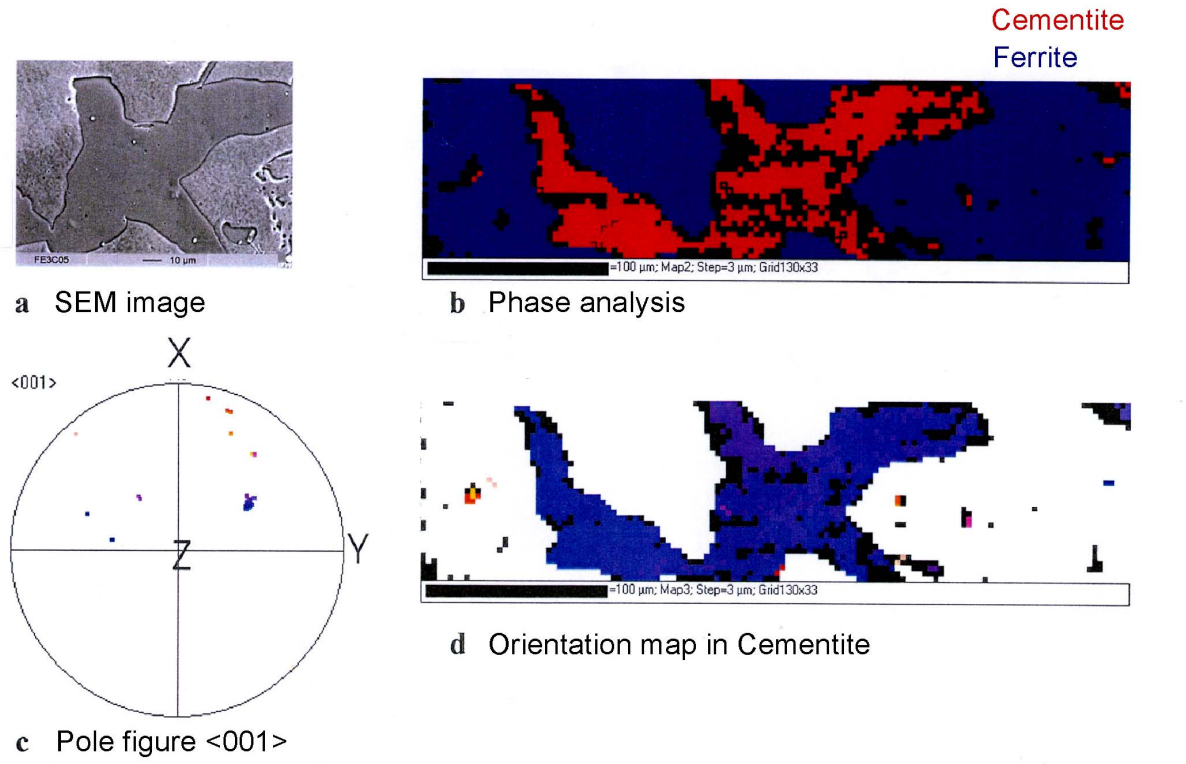

Figure 10: (a) Secondary electron micrograph, (b) phase map, (c) pole figure and, (d) orientation maps.

The Kikuchi method had therefore established that the specimen contained two phases (ferrite and cementite) and that the cementite phase consists of fairly large single crystals (>10 µm). Electron diffraction methods are however less accurate than X-ray methods. Since the cementite phase has been established as being a single crystal with 20 – 50 µm diameter grains this allows use of the KOSSEL-technique for the identification of the phases. If it had contained grains with different orientation, a highly resolving micro diffractometer would have been required.

6.1.2.2 Application of the KOSSEL-Technique

The KOSSEL-technique is a micro-X-ray diffraction method, in which the X-ray source is generated in the specimen (crystal) itself. The generated X-radiation (characteristic X-rays) is diffracted by the crystal lattice of the same crystal or grain. The basic requirement is that the micro-volume under investigation must be a single crystal. The diffraction pattern, the so-called KOSSEL-diagram, of each single crystal is an individual fingerprint of the structure and orientation of this crystal. Even for different phases with identical crystal structure, but slightly different lattice parameters the positions of KOSSEL cones in the pattern are shifted. Thus, identification of phases by this technique is more sensitive and also more reliable than with the reflection-KIKUCHI technique [11].

In the present case a Fe-Kα a source was generated inside the grains by an electron beam in an SEM, but at beam currents higher than usual in the SEM. The emerging diffraction cones were recorded on a highly sensitive film or by a CCD-camera as shown in Figure 11 and 12. Most important for the characterization are those cones with small radii, i.e. small solid angles. These cones appear in the projection plane of the image as circles or circle segments. Such a system of circles (reflexes, KOSSEL lines) is characteristic for the corresponding phase. In the present case the circles clearly could be attributed to reflections of Fe (Figure 11) and Fe_3C (Figure 12).

The width of the lines is a measure for internal stresses. It turns out that in the present case that the ferrite phase in the pearlite seem to be highly stressed, as expected, (Figure 11a) as indicated by the rather diffuse lines in comparison with an Fe-single crystal with a similar orientation (Figure 11b) which has very sharp lines. The Fe_3C-grains have less stress. Their lines are sharp (Figures 12a and 12b).

The two patterns from different cementite grains (Figure 12) were identified by lattice indices, which were compared to the lattice structure of Fe_3C obtained from Meinhardt and Krisement works [14].

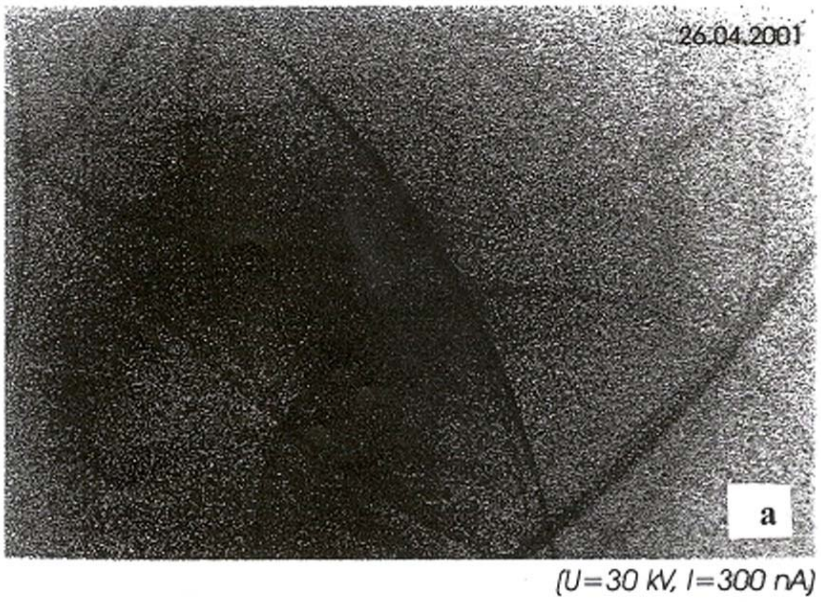

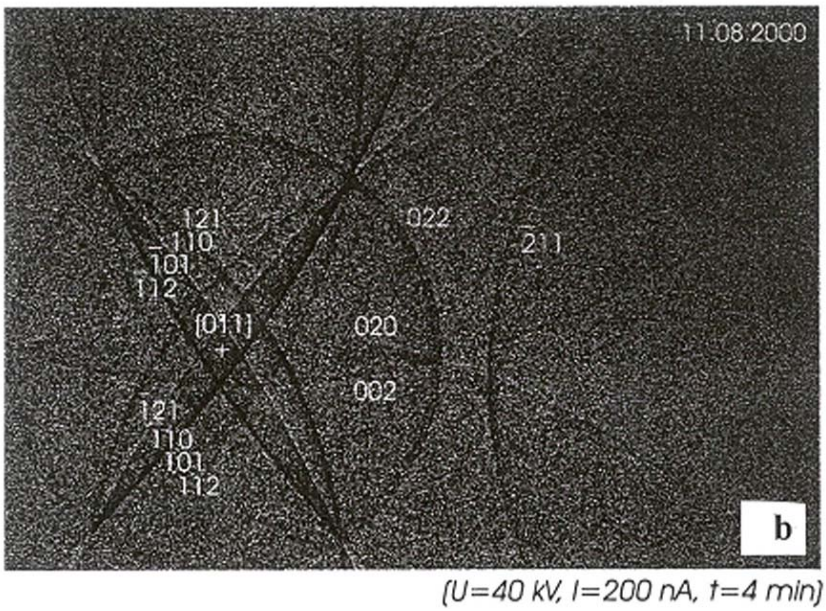

Figure 11: Kossel diffraction patterns from pure iron, "a" pattern from a small iron grain in CRM, "b" pattern from single Fe(100) crystal.

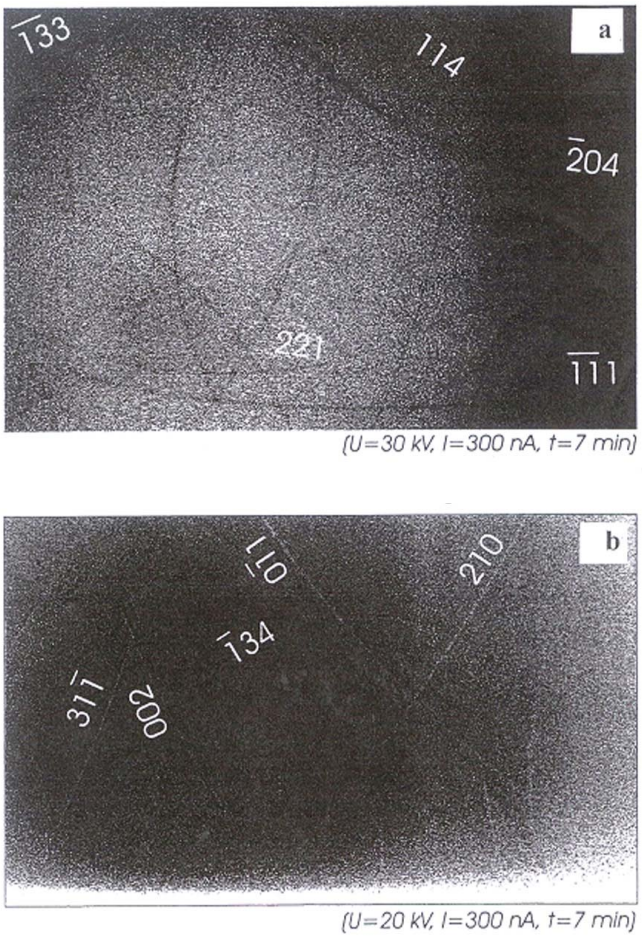

Figure 12: Kossel diffraction patterns from Cementite phases in the CRM.

6.1.3 Summary

The thermodynamic Fe-C phase diagram shows that cementite is a line compound with a unique stoichiometric composition (Fe_3C). The presence of cementite in the proposed CRM was demonstrated by conventional X-ray diffraction along with ferrite (section 6.1.1). Further confirmation that the specimen has a two-phase structure was provided by Kikuchi electron diffraction patterns in an SEM (section 6.1.2.1). Furthermore, the cementite grains were single crystal (section 6.1.2.1). This allowed the Kossel micro X-ray diffraction method to be used and provided direct confirmation that the individual grains within the specimen were indeed cementite (section 6.1.2.2). The identification of the cementite phase is unambiguous. The cementite grains mostly are single-crystal, but contain some small angle grain boundaries.

In conclusion, the crystallographic structure of the carbide is completely consistent with the line compound Fe_3C. This compound has a high degree of stoichiometry (Fe_3C) with an established and accepted value for the carbon atom fraction: 0.25 carbon atom in Fe_3C and carbon mass fraction of 66.9 g/kg. The value is directly derived from the stoichiometry of Fe_3C: 3 atoms of iron for 1 atom of carbon.

Table 6: Certified value for carbon in cementite grains derived from Fe_3C stoichiometry.

	Carbon atom fraction [mol/mol]	Carbon mass fraction [g/kg]
Certified value	0.25	66.9

6.2 Confirmation by atom probe tomography analysis

3D-atom probe tomography (3D-APT) was used by one laboratory to confirm the stoichiometry of Fe_3C in single grain of cementite by the direct measurement of the carbon mass fraction [15].

Method used

3D-atomic probe tomography, commonly referred to as 3D-atomic probe, is a technique, which involves the atom-by-atom dissection of a small volume of a material. Specimens are in the form of sharply-pointed needles, with an end radius less than 100 nm. These specimens are subjected to cryogenic temperatures (~100 K) and high voltage (~10 kV), causing the atoms at the apex of the very sharp specimen tip to ionize and accelerate away from the positively-charged tip and towards a detector. The small radius of curvature at the end of the tip causes a diverging electrical field, resulting in a natural magnification of ions field-evaporated from it, allowing for resolution on the atomic scale.

A two-dimensional position-sensitive detector is used to identify from where on a tip's surface an ion originated. As atoms on the tip are field-evaporated, the layers beneath the surface are exposed; the sequence of field-evaporated ions is used to reconstruct the third dimension.

The detector records both the ion's time-of-flight (and hence its mass-to-charge ratio - its chemical identity) and its impact position (and hence its original location on the tip surface prior to ionization). A typical 3D-APT run records on the order of 500,000 ion times and positions. These data are analyzed by specific software that allows the reconstruction of all atomic positions within the analytical volume (typically of the order of 10 x 10 x 100 nm).

Knowing the number of carbon atoms detected and the total number of atoms seen by the detector, the percentage of carbon atoms is easily determined as the atom evaporation is not atom specific.

Study set-up

APT measurements were performed by one laboratory. Three specimens were selected randomly and 2 – 3 point analyses were made on different samples of each specimen. The analyses were done on different days in a randomised order. The average number of atoms counted was 600000 per analysis. The analytical setup is detailed in Annex D.

In order to verify the performance of the equipment, the isotopic ratios ^{13}C / ^{12}C and ^{54}Fe / Fe_{total} were compared to the natural isotope abundance. The relative isotopic abundance measured for ^{13}C (1.11 ± 0.09) % and ^{54}Fe (5.82 ± 0.06) % were in good agreement with the accepted natural values for ^{13}C: 1.07 % and for ^{54}Fe: 5.845 % [16].

Evaluation of results

The data obtained were first checked for compliance with the requested analysis protocol and for their validity based on technical reasons. The following criteria were considered during the evaluation:

- compliance with the analysis protocol: sample preparations and measurements performed on several days.
- correctness of the measurements based on knowledge of the method
- absence of values given as below the limit of detection or below limit of quantification

Based on the aforementioned criteria the dataset was considered as technically valid.

Individual results for the confirmation study together with the uncertainty stated by the laboratory are reported in Annex E.

Comparison of APT results with the certified value

For confirming the assigned value of carbon mass fraction, the measured values of carbon in Fe_3C grains in 2 different specimens of IRMM-471 are compared with the certified value. The absolute difference between mean measured value and the certified value was determined as Δ_m. The measurement uncertainty (u_m) with the uncertainty of the certified value (u_{CRM}) was used to determine the uncertainty of the difference between the certified value and the confirmatory results: $u_\Delta = \sqrt{u_m^2 + u_{CRM}^2}$. Then the expanded uncertainty (U_Δ) is calculated from the combined uncertainty (u_Δ) using a coverage factor of 2, corresponding to a level of confidence of approximately 95 %: $U_\Delta = 2 \cdot u_\Delta$

Table 7: Results of the confirmation analysis; comparison between the certified value based on stoichiometric assessment and results of direct carbon analysis by APT.

	Carbon atom fraction from APT results [mol/mol]	**Carbon certified value [mol/mol]**
Mean value of carbon atom fraction (number of measurements = 8)	0.249	0.25
Standard deviation of the measurements	0.005	
Measurement uncertainty (k factor = 1)	0.002	0.005
	Results of comparison carbon atom fraction [mol/mol]	
Δ_m	0.001	
U_Δ (k factor = 2)	0.010	

As $\Delta_m \leq U_\Delta$, there is no significant difference between the confirmation measurement and the certified value, at a confidence level of about 95 %. A comparison of the variance from APT analysis and from the certified value uncertainty did not show any significant difference using F-test at 95 % of confidence level.

The direct measurement of carbon mass fraction in cementite grains confirmed the certified carbon mass fraction value, which was calculated on the basis of thermodynamic proof of stoichiometry.

6.3 Verification measurements

Saunders et al. [17] studied the linearity of the relationship between the measured counts and carbon concentration of IRMM-471 referred to as BCR-726 in their study. This relationship was validated experimentally with an inter-comparison between 9 different laboratories in which a set of C-containing steels and a pure iron were used together with the IRMM-471 specimen. The compositions of the steels used in the set were verified using three different analysis methods in at least two different laboratories [17]. Regression analysis of all results indicated an average coefficient of determination of 0.9999 confirming a linear relationship between measured counts and carbon concentration for C values between less than 10 g/kg to 67 g/kg.

6.4 Uncertainty budget

The assigned value is derived from the stoichiometry of Fe_3C. Literature does not provide an uncertainty value for the stoichiometry of cementite. However, the confirmation analysis by APT clearly showed that the assigned value (carbon mass fraction = 66.9 g/kg) agrees with independent measurements done by APT (Δ_m is more than 10 times lower than U (k = 2)) taking into account the homogeneity uncertainty as total uncertainty. The decision was made

to estimate an uncertainty for the carbon mass fraction by assuming the data (assigned value from Fe_3C stoichiometry and APT results) follow a rectangular distribution. For such distribution, a relative standard uncertainty ($u_{char,rel}$) can be estimated using the following formula:

$$u_{char,rel} = \frac{\left|\bar{y}_{APT} - \bar{y}\right|}{\sqrt{3} \times \bar{y}} \times 100 \qquad \textbf{Equation 4}$$

where:

$\bar{y}$ = assigned value derived from Fe_3C stoichiometry

$\bar{y}_{APT}$ = mean value of APT results

Table 8: Calculation of $u_{char,rel}$ for carbon mass fraction in cementite grain using rectangular distribution model.

	Results
Carbon mean value from APT measurements [mol/mol]	0.249
Carbon assigned value derived from Fe_3C stoichiometry [mol/mol]	0.250
$u_{char,\ rel}$ [%]	0.2

The evaluation of u_{char} was done in a conservative way and shows a $u_{char,rel}$ representing less than 10 % of the total uncertainty.

The Fe-C phase diagram, based on numerous thermodynamic and crystallographic data, indicates that Fe_3C is a line compound with a well defined stoichiometry, which has been verified in the characterisation section. However, interstitial or substitutional lattice defects or vacancies can occur. Different models have been used in the literature [18] to estimate the effect of Fe-vacancies or C-vacancies on the Fe_3C equilibrium elemental composition. These models can be used to consider the presence of vacancies, which has not been checked in the cementite grains of IRMM-471 samples. The Fe-vacancies model gives a composition of carbon equal to (66.9 ± 0.02) g/kg and the C-vacancies model gives a composition of carbon equal to (66.5 ± 0.2) g/kg. A conservative combination of the effects of the two vacancy types gives a mass fraction of carbon equal to (66.5 ± 0.2) g/kg, which represents a relative difference of 0.6 % with the assigned value. The comparison of the carbon mass fraction in cementite considering the combined vacancies model (66.5 ± 0.2) g/kg with the assigned values and u_{char} (66.9 ± 0.13) g/kg shows agreement for a coverage factor k = 2. It is noted that the final step in the IRMM-471 thermal process of production is a slow cooling, which minimizes the possible level of lattice defects or vacancies by diffusion and cross-elimination. The minimization of possible lattice defect or vacancies minimize the uncertainty expected for the assigned value. This therefore confirms the defined stoichiometry of the cementite phase in IRMM-471.

For the above reasons, the calculated u_{char} was considered to be representative, and because of its small value it was assumed to be negligible in comparison to u_{bb}.

7 Value Assignment

For these materials, certified values have been assigned.

7.1 Certified values and their uncertainties

The certified values are based on the stoichiometry of Fe_3C confirmed by single phase identification and direct measurement by an independent method.

The assigned uncertainty consists of uncertainties related to characterisation, u_{char} (see section 6), potential between-unit inhomogeneity, u_{bb} (see section 4) and potential degradation during transport (u_{sts}) and long-term storage, u_{lts} (see section 5). These different contributions were combined to estimate the expanded, relative uncertainty of the certified value ($U_{CRM,\,rel}$) with a coverage factor k as:

$$U_{CRM,rel} = k \cdot \sqrt{u_{char,rel}^2 + u_{bb,rel}^2 + u_{sts,rel}^2 + u_{lts,rel}^2}$$

- u_{char} was estimated as described in Section 6.4.
- u_{bb} was estimated as described in Section 4.1.
- u_{sts} was estimated as described in Section 5.3.
- u_{lts} was estimated as described in Section 5.3. As demonstrated in section 5, Fe_3C is stable at ambient conditions so the uncertainty of degradation during storage may have been considered negligible.

Because of the sufficient numbers of the degrees of freedom of the different uncertainty contributions, a coverage factor k = 2 was applied, to obtain the expanded uncertainties. The certified value and its uncertainty is given in Table 9.

Table 9: Certified value and their uncertainties for CRM

Property	Certified value [g/kg]	$u_{sts,\,rel}$ [%]	$u_{lts,\,rel}$ [%]	$u_{bb,\,rel}$ [%]	$u_{char,\,rel}$ [%]	$U_{CRM,\,rel}$ [%]	U_{CRM} [g/kg]
Carbon	66.9	0.18	0.31	1.95	0.20	3.98	2.7

This shows that in fact the main contributor of uncertainty is the potential between-unit inhomogeneity. It represents 98 % of the total uncertainty.

8 Metrological traceability and commutability

8.1 Metrological traceability

Identity

Structurally defined: Carbon is a chemically clearly defined analyte. The participants used different methods for the sample preparation as well as for the final determination, demonstrating the absence of measurement bias. The measurand is therefore structurally defined and independent of the measurement method.

Quantity value

Traceable to SI: Different calibrants were used and all relevant input parameters were calibrated. Instruments in individual laboratories were verified and calibrated with tools ensuring traceability to the SI. As the assigned value is combination of agreeing results individually traceable to the SI, the assigned quantity value itself is traceable to the SI as well.

9 Instructions for use

9.1 Storage conditions

The materials shall be stored at 18 °C ± 5 °C in a laboratory desiccator. Care shall be taken to avoid exposure of the sample to humidity once the sample box is opened. The specimens should be only removed for the duration of the tests.

Please note that the European Commission cannot be held responsible for changes that happen during storage of the material at the customer's premises, especially of opened samples.

9.2 Safety and protection for the environment

The usual laboratory safety measures apply.

9.3 Preparation and use of the material

The CRM consists of a transverse section of 5 mm diameter taken from a 4 - 5 mm long rod. The microstructure of the rod comprises ferrite, pearlite and massive cementite grains. Some decarburisation was evident around the circumference of this rod, therefore, the traverse section contains numerous carbides up to approximately 150 micrometres in size. Nevertheless the composition of the carbides is the same irrespective of position. The carbon mass fraction equals (66.9 ± 2.7) g/kg (expanded uncertainty k = 2).

To visualize the Fe_3C phase, several techniques are available. Fe_3C particles are visible optically as orange/yellow areas after polishing (Figure 13). Moreover they can be easily spotted in the electron probe microanalyser (EPMA) using either the secondary electrons or backscattered electrons signal.

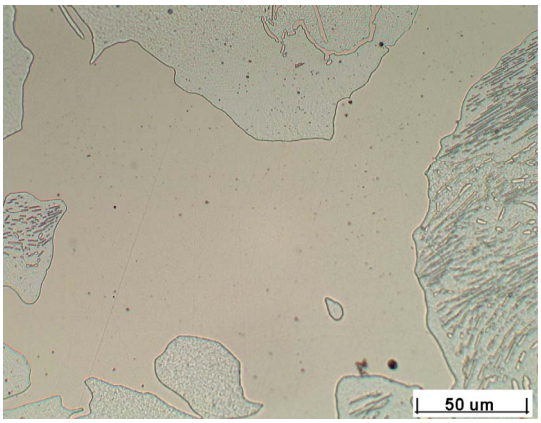

Figure 13: Optical micrograph showing appearance of Fe_3C

It is recommended that the following procedure is followed before each examination of the CRM.

1. Polish for a maximum of 30 seconds using 0.05 µm γ-Alumina on a hard cloth, lubricated using de-ionized water
2. Clean in ultrasonic bath for 5 minutes using acetone
3. Repeat cleaning using ethanol
4. Optional final ultrasonic clean using distilled water
5. Dry carefully so as to avoid drying stains.
6. Demagnetize

If the prepared surface of the CRM becomes scratched, it should be re-prepared using diamond impregnated pads with hard cloths with an oil-based lubricant and finished using the

above method. Check for rounding of the individual carbides by examining optically at a low magnification.

The CRM should be placed ideally in the instrument at least 16 hours (overnight) before examination. Insertion of the specimen into the EPMA the day prior to examination was found to be beneficial as regards contamination - due to desorption of hydrocarbons from the specimen surface.

It is recommended that the central region of a cementite grain in the CRM is analysed using the following parameters:

Table 10: Analytical parameters recommended for EPMA measurements.

Acceleration voltage	10 kV
Beam current	100 nA
Beam condition	Focused spot
Decontamination time	Appropriate for the individual instrument (~ 10 s)
Pulse height analyser settings	Optimized values of baseline, window width, gain and detector bias
Count time	Sufficient to collect over 10,000 counts (required for 1 % relative error)
No. of repeats	At least 3 statistically consistent readings

The value of the background should be determined by prior examination of a pure iron calibrant prepared and examined using the same method as described above. Further guidance on analysis methodology is given in Appendix G.

9.4 Minimum sample intake

The minimum sample intake representative for carbon mass fraction is 0.000024 μm^3.

9.5 Use of the certified value

The main purpose of these materials is for calibration and to assess method performance, i.e. for checking accuracy of analytical results/calibration. As any reference material, it can also be used for control charts or validation studies.

Comparing an analytical result with the certified value

A result is unbiased if the combined standard uncertainty of measurement and certified value covers the difference between the certified value and the measurement result (see also ERM Application Note 1, www.erm-crm.org [19].

For assessing the method performance, the measured values of the CRMs are compared with the certified values. The procedure is briefly described here:

- Calculate the absolute difference between mean measured value and the certified value (Δ_m).
- Combine measurement uncertainty (u_m) with the uncertainty of the certified value (u_{CRM}): $u_\Delta = \sqrt{u_m^2 + u_{CRM}^2}$
- Calculate the expanded uncertainty (U_Δ) from the combined uncertainty ($u_{\Delta,}$) using an appropriate coverage factor, corresponding to a level of confidence of approximately 95 %
- If $\Delta_m \leq U_\Delta$ then there is no significant difference between the measurement result and the certified value, at a confidence level of about 95 %.

Use as a calibrant

If used as a calibrant, the uncertainty of the certified value shall be taken into account in the estimation of the measurement uncertainty.

Use in quality control charts

The materials can be used for quality control charts. Different CRM-units will give the same result as inhomogeneity was included in the uncertainties of the certified values.

Acknowledgments

The authors would like to thank Gert Roebben and James Snell (IRMM) for the reviewing of the certification report, as well as the experts of the Certification Advisory Panel "Element", Steve Balsley (International Atomic Energy Agency, AT), Thomas Prohaska (University of Natural Resources and Life Sciences, AT) and Peter Vermaercke (Studiecentrum voor Kernenergie, SCK, BE) for their constructive comments.

Most of the work described in this project was part of the European project Electron-probe MICROanalysis of LIghT Elements; Measurement Methods and Certified Reference Materials, (MICROLITE) - EC Contract No. SMT4-CT98-2210) which was focused on the microanalysis of carbon and nitrogen. The authors would like to thank MICROLITE for funding and supporting the project.

The authors would like to acknowledge Dr Maurice Cox from NPL and Dr Eulogio Pardo from Leeds University for their help in the statistical treatment of the data.

References

1 ISO/IEC Guide 98-3, Uncertainty of measurement -- Part 3: Guide to the expression of uncertainty in measurement (GUM:1995), International Organization for Standardization, Geneva, Switzerland, 2008.

2 ISO 16592 - Microbeam analysis - Electron probe microanalysis - Guidelines for determining the carbon content of steels using a calibration curve method, International Organization for Standardization, Geneva, Switzerland, 2006.

3 ISO 22489 - Microbeam analysis - Electron probe microanalysis - Quantitative point analysis for bulk specimens using wavelength-dispersive X-ray spectroscopy, International Organization for Standardization, Geneva, Switzerland, 2006.

4 G.F. Bastin, H.J.M. Heijligers, Quantitative Electron Probe Microanalysis of Carbon in Binary Carbides. University of Eindhoven. The Netherlands, (1990).

5 O. Kubaschewski, Iron-Binary Phase Diagrams, Springer-Verlag, Berlin, Germany, (1982).

6 P. Gustavson, A Thermodynamic Evaluation of the Fe-C System, Scand. J. Metall. 14[5] (1985) 259-267.

7 ISO Guide 34, General requirements for the competence of reference materials producers, International Organization for Standardization, Geneva, Switzerland, 2009.

8 ISO 14595 - Microbeam analysis - Electron probe microanalysis - Guidelines for the specification of certified reference materials (CRMs), International Organization for Standardization, Geneva, Switzerland, 2003.

9 T.P.J. Linsinger, J. Pauwels, A. Lamberty, H. Schimmel, A.M.H. van der Veen, L. Siekmann, Estimating the Uncertainty of Stability for Matrix CRMs, Fres. J. Anal. Chem. 370 (2001) 183-188.

10 A.J. Schwartz, M. Kumar, B.L. Adams (Eds.), Electron Backscatter Diffraction in Materials Science, Kluwer Academic/Plenum Publications, New York, US, (2000).

11 S. Däbritz, E. Langer, W. Hauffe, Kossel and pseudo Kossel CCD pattern in comparison with electron backscattering diffraction diagrams, Appl. Surf. Sci. 179 [1–4] (2001) 38-44.

12 JCPDS International Centre for Diffraction Data (JCPDS-ICDD 2000) PDF number 06-0696, Swanson et al., Natl. Bur. Stand. (US), Circ. 539, IV, 3 (1955).

13 JCPDS International Centre for Diffraction Data (JCPDS-ICDD 2000) PDF number 35-0772, Natl. Bur. Stand. (US) Monogr. 25, 21, 72 (1985).

14 D. Meinhardt, O. Krisement, Strukturuntersuchungen an Karbiden des Eisens, Wolframs und Chroms mit Thermischen Neutronen, Arch. Eisenhuttenwes 33[7] (1962) 493-499.

15 R.C. Thomson, Characterization of Carbides in Steels Using Atom Probe Field-Ion Microscopy, Mater. Charact. 44[1–2] (2000) 219-233.

16 K.J.R. Rosman, P.D.P. Taylor, Isotopic compositions of the elements 1997 (Technical Report), Pure Appl. Chem. 70 (1998) 217-235.

17 S. Saunders, P. Karduck, W.G. Sloof, Certified Reference Materials for Micro-Analysis of Carbon and Nitrogen, Microchim. Acta, 145 (2004) 209-213.

18 F. Kayser, Y. Sumitomo, On the composition of cementite in equilibrium with ferrite at room temperature. Journal Phase Equil., 18[5] (1997) 458-464.

19 T.P.J. Linsinger, ERM Application Note 1: Comparison of a measurement result with the certified value, www.erm-crm.org (last accessed on 13/10/2012)

20 ISO 14595 - Microbeam analysis - Electron probe microanalysis - Guidelines for the specification of certified reference materials (CRMs), International Organization for Standardization, Geneva, Switzerland, 2003.

21 M. G. Kendall, A. Stuart. The Advanced Theory of Statistics. Volume 3: Design and Analysis, and Time-Series. Charles Griffin and Co. (Eds), London, UK (1966).

Annexes

Annex A: Results of the homogeneity measurements

Table A1: Summary of the methods used for the homogeneity study

Instrument	Energy [keV]	Current [nA]	Count time [s]	Decontam.	Decontam. time [s]	Remarks
fully automated CAMEBAX SX 50 EPMA with four wavelength-dispersive (WD) spectrometers	10	200	15	L-N_2 trap and O_2 jet	15	• Focused electron beam • C-Kα background intensity obtained on pure iron under the same condition at the beginning and at the end of the total run. • Fe-Kα measured with another wavelength-dispersive spectrometer (LiF-crystal), simultaneously with measurement of C-Kα.

Figure A1: Carbon counts for the samples tested in the homogeneity study (error bars represent the standard deviation of the 50 points analysis made on each sample)

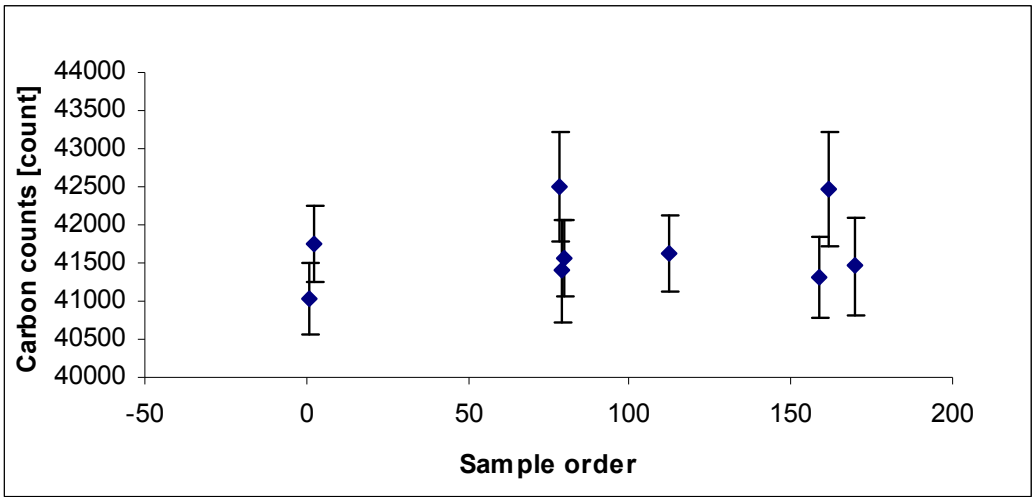

Figure A2: Rod position homogeneity (error bars represent the standard deviation of the 50 points analysis made on each sample)

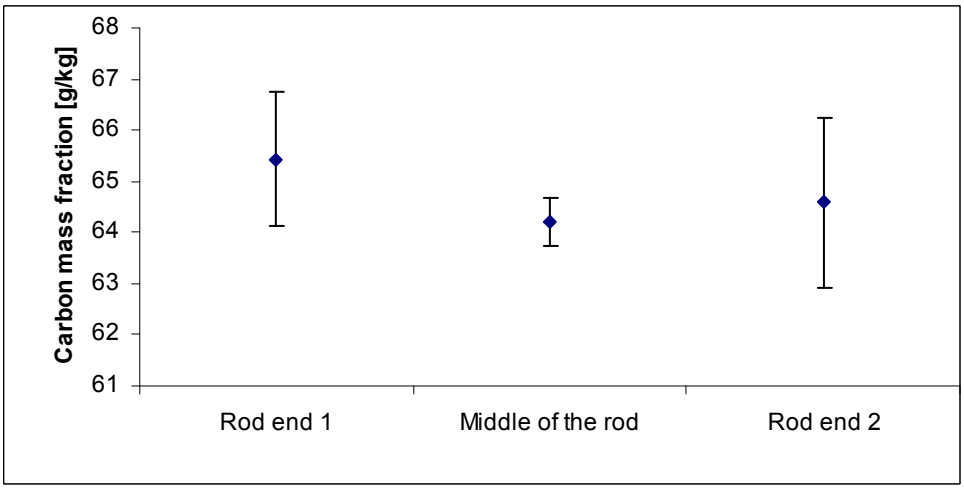

Annex B: Results of the short-term stability measurements

Table B1: Carbon analysis of Fe_3C specimens for temperature stability tests. EPMA analysis on 50 points.

Test	Time [week]	Mean value [g/kg]	Standard deviation [g/kg]	Standard deviation of the mean value [g/kg]	Number of analysis
Reference conditions	0	66.59	0.91	0.13	50
Temperature stability (-50 °C and +110 °C)	2	66.77	0.66	0.09	50
Temperature stability (-50 °C and +110 °C)	2	67.22	0.43	0.06	50

Table B2: Carbon analysis of Fe_3C specimens for humidity and UV radiation stability tests. EPMA analysis on 50 points.

Test	Time [week]	Mean value [g/kg]	Standard deviation [g/kg]	Standard deviation of the mean value [g/kg]	Number of analysis
Reference conditions	0	66.59	0.91	0.13	50
50 % humidity and UV radiation of 50 W/m²	12	66.77	0.66	0.09	50
12 % humidity and UV radiation of 50 W/m²	12	66.27	0.48	0.07	50

Annex C: Results of the long-term stability measurements

Figure C1: Graphic of stability results over 120 months (error bars represent the standard deviation of the measurements done on each sample).

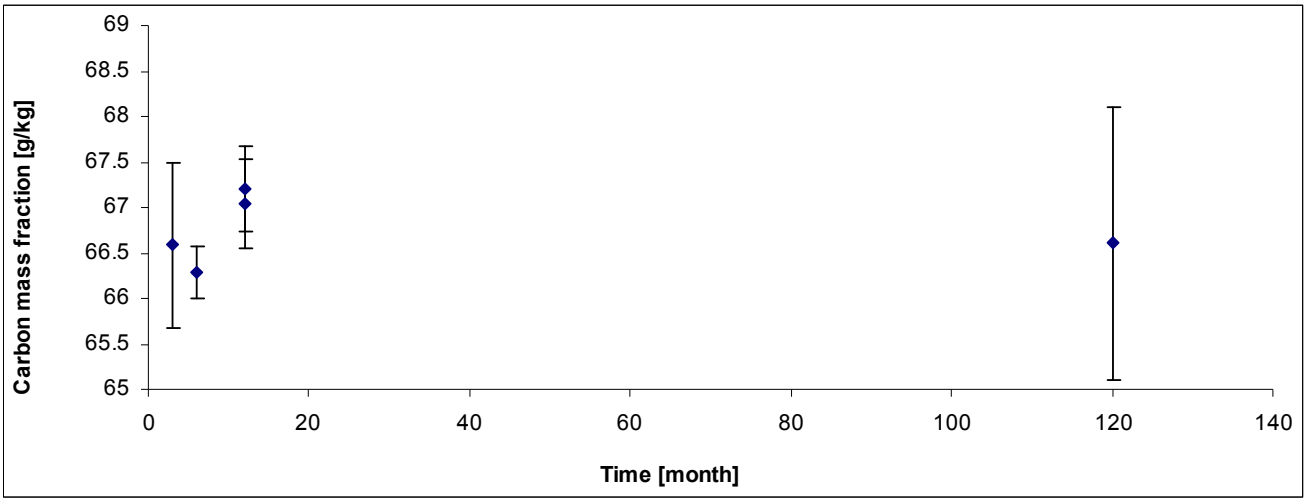

Table C1: Results of the long term stability study

Time [month]	Mean [g/kg]	Standard deviation [g/kg]	Number of measurements	Standard deviation of the mean [g/kg]	Method
3	66.59	0.91	50	0.13	EPMA
6	66.29	0.28	50	0.04	EPMA
12	67.05	0.49	50	0.07	EPMA
12	67.21	0.48	50	0.07	EPMA
120	66.60	1.50	8	0.53	APT

Annex D: Summary of methods used in the characterisation

Table D1: Method used for phase identification by XRD

Parameter	Instrument	Scan range [2θ]	Step size	Count time [s]	measurement method
Diffraction angles corresponding with lattice planes	Siemens D500 X-ray powder diffractometer system,(θ-2θ geometry)	20^{o} to 160^{o}	0.02^{o}	20	XRD with Cr-Kα radiation

Table D2: Method used for atom probe tomography

Parameter	Instrument	Operations	Final sample
Sample preparation for APT measurement	Focussed Ion Beam (Ga+ source) FEI quanta 300 Dualbeam	Pt deposit Annular FIB milling	Bar-shaped base specimen 30 µm x 3 µm x 3 µm Pt deposit: 30 µm x 3 µm x 1 µm

Parameter	Instrument	Detector	Pulse	Atoms counted and rate of detection	measurement method
Number of carbon atoms	ECOTAP (CAMECA)	Advanced delay line detector and a wide angle reflectron	pulse fraction 20 %, pulse repetition rate 30 kHz	250000 to 800000 (rate of detection: 45 %)	APT on sample kept at temperature 100 K. The following ions were used for the determination of C mass fraction: C^{2+}, C^{+}, C_3^{2+}, C_2^{+}, C_4^{2+}, C_3^{+}, C_4^{+} ratio C_4^{2+}/C_2^{+} based on natural isotopic ratio of ^{12}C and ^{13}C

Annex E: Results of the characterisation measurements

Table E1: Atom Probe Tomography results. Carbon atom fraction in cementite was measured using APT technique. APT measurements (8 replicates in total) were performed by 1 laboratory on 3 specimens and on different days. The standard deviation of the measurement is given as reported by participating laboratory (k = 1). The results from APT were converted from [mol/mol] into [g/kg] considering the presence of iron and carbon only.

Replicate from one laboratory	**carbon atom fraction [mol/mol]**	**Standard deviation of the measurement [mol/mol]**	**Converted carbon mass fraction [g/kg]**	**Converted Standard deviation of the measurement in [g/kg]**
1	0.242	0.0005	64.25	0.11
2	0.253	0.0005	67.90	0.11
3	0.243	0.0005	64.58	0.11
4	0.248	0.001	66.23	0.22
5	0.253	0.0005	67.90	0.11
6	0.252	0.0005	67.56	0.11
7	0.249	0.0005	66.56	0.11
8	0.253	0.0005	67.90	0.11
Average	0.249		66.60	
Standard deviation	0.005		1.50	

Annex F: Statistical analysis, description of the microprobe data analysis

1 Introduction

A description of the calculations performed in the statistical analysis of measurements of certified reference materials gathered using electron probe microanalysis is given. It is based on ISO 14595 [20]. The statistical analysis has been extended to integrate the specimens prepared from a number of production batches of material.
The statistical analysis of the data for homogeneity study has been done through three-way hierarchical classification ANOVA. The statistical analysis was developed by Maurice Cox and Eulogio Pardo and a specially designed and tested EXCEL spreadsheet was used for the statistical analysis. The following annex details the statistical analysis as it has not been published.

The analysis can be seen as consisting of three stages:

1. Pre-process the measurement data to a form suitable for standard Analysis of Variance (ANOVA).

2. Perform ANOVA on the pre-processed data.

3. Post-process the ANOVA results to provide the required measurement results.

The experimental design is as follows. The Certified Reference Material (CRM) contains a carbon to be analysed. The CRM is divided into a number of production batches (3 production batches). Each batch is divided into a number (the same number) of specimens (3 specimens from each production batch). A number of points (the same number) are taken on each specimen (104 points from each specimen). Only one measurement is taken at each point.

Define

n_E = number of elements,
n_B = number of production batches,
n_S = number of specimens,
n_P = number of points,
n_R = number of replicates.

For the method of analysis n_S, n_P and n_R must all be two or greater. The number of elements, n_E, and the number of batches, n_B, may be one or greater.

Then the total number of measurements (over all replicates) is $n_B \times n_S \times n_P \times n_R$.

Individual replicate measurements are referenced by four indices:
b = production batch index,
s = specimen index,
p = point index,
r = replicate index.

These indices, being the initial letter in “batch”, “specimen”, etc. are used in preference to those in the standard. Also, an additional index was required to denote “production batch”.

2 Measurement data

The measured data consists of the following items:

1. A value for the certified mass fraction $\hat{W}_0$.

2. A value for the reference current I_0.

3. For each element:

(a) Integrated X-ray count values

$$Y_{bspr},\ b = 1, \ldots, n_B,\ s = 1, \ldots, n_S,\ p = 1, \ldots, n_P,\ r = 1, \ldots, n_R.$$

The value Y_{bspr} represents the r^{th} replicate count measured at point p of specimen s in production batch b.

(b) Background-count values (The notation G is used for background count (G for "ground" in "background") to avoid a notational clash with "B" for batch.). These are specified in either of the following two forms:

i. Values

$$G_{bspr},\ b = 1, \ldots, n_B,\ s = 1, \ldots, n_S,\ p = 1, \ldots, n_P,\ r = 1, \ldots, n_R$$

corresponding to the provided values of Y_{bspr}.

ii. Values

$$G_g,\ g = 1, \ldots, m_G.$$

In the former case a background count measurement is made corresponding to each value of Y_{bspr}. In the latter case a set of m_G background count measurements are made in a manner less associated with the individual Y_{bspr}.

(c) Measured current values

$$I_{bspr},\ b = 1, \ldots, n_B,\ s = 1, \ldots, n_S,\ p = 1, \ldots, n_P,\ r = 1, \ldots, n_R$$

corresponding to the values of Y_{bspr}.

3 Data analysis

Uncertainties in the element concentrations result from inhomogeneity across batches and within specimens and between specimens and in the data acquisition during the test. These uncertainties can be determined from the use of a statistical procedure known as ANOVA (Analysis of Variance). A convenient way to carry out this analysis is to apply the three-stage process.

3.1 Pre-processing

Just one item of pre-processing is necessary. The measured counts Y_{bspr} are corrected for current drift. Specifically, each value of

$$Y_{bspr},\ b = 1, \ldots, n_B,\ s = 1, \ldots, n_S,\ p = 1, \ldots, n_P,\ r = 1, \ldots, n_R$$

is replaced by

$$Y_{bspr} \times I_0 / I_{bspr}.$$

In an implementation, the provided values of Y_{bspr} are retained to maintain a record of the input data.

3.2 Analysis of variance

In the terminology of ANOVA the measurement procedure is known as a *design*, consisting of groups, sub-groups, etc. The batches relate to the groups, the specimens to sub-groups, the points to sub-sub- groups, with the replicate measurements forming the data in the sub-sub-groups. The design is a three-way hierarchical classification or, since there are an equal number of replicate measurements in each group at the lowest level, a three-way nested classification [21]. The mean value at each point within each specimen in each batch, i.e., with respect to the replicate measurements at that point, is

$$Y_{bsp.} = \sum_{r=1}^{n_R} Y_{bspr}/n_R, \quad b = 1, \ldots, n_B, \quad s = 1, \ldots, n_S, \quad p = 1, \ldots, n_P,$$

The mean value for each specimen in each batch, i.e., with respect to the replicate measurements at the points within that specimen, is

$$Y_{bs..} = \sum_{p=1}^{n_P} Y_{bsp.}/n_P, \quad b = 1, \ldots, n_B, \quad s = 1, \ldots, n_S,$$

The mean value for each batch, i.e., with respect to the replicate measurements at the points within the specimens in that batch, is

$$Y_{b...} = \sum_{s=1}^{n_S} Y_{bs..}/n_S, \quad b = 1, \ldots, n_B,$$

and the overall mean, i.e., with respect to the replicate measurements at the points within the specimens in the batches, is

$$Y_{....} = \sum_{b=1}^{n_B} Y_{b...}/n_B.$$

The measurement model is

$$Y_{bspr} = \bar{Y} + B_b + S_{bs} + P_{bsp} + R_{bspr}$$

or, equivalently (*cf.* [2, p12]),

$$Y_{bspr} - Y_{....} = (Y_{b...} - Y_{....}) + (Y_{bs..} - Y_{b...}) + (Y_{bsp.} - Y_{bs..}) + (Y_{bspr} - Y_{bsp.}),$$

where

$\bar{Y}$ = $Y_{....}$ = overall mean value,
$B_b = Y_{b...} - Y_{....}$ = differential effect of the b_{th} batch,
$S_{bs} = Y_{bs..} - Y_{b...}$ = differential effect of the s_{th} specimen from the b_{th} batch,
$P_{bsp} = Y_{bsp.} - Y_{bs..}$ = differential effect of the p_{th} point within the s_{th} specimen from the b_{th} batch,
$R_{bspr} = Y_{bspr} - Y_{bsp.}$ = residual error of the r_{th} replicate measurement taken at the p_{th} point within the s_{th} specimen from the b_{th} batch.

Taking sums of squares of each side over all measurement indices,

$$\sum_{b=1}^{n_B}\sum_{s=1}^{n_S}\sum_{p=1}^{n_P}\sum_{r=1}^{n_R}(Y_{bspr}-Y_{....})^2 = \sum_{b=1}^{n_B}\sum_{s=1}^{n_S}\sum_{p=1}^{n_P}\sum_{r=1}^{n_R}(Y_{b...}-Y_{....})^2+\sum_{b=1}^{n_B}\sum_{s=1}^{n_S}\sum_{p=1}^{n_P}\sum_{r=1}^{n_R}(Y_{bs..}-Y_{b...})^2$$
$$+ \sum_{b=1}^{n_B}\sum_{s=1}^{n_S}\sum_{p=1}^{n_P}\sum_{r=1}^{n_R}(Y_{bsp.}-Y_{bs..})^2+\sum_{b=1}^{n_B}\sum_{s=1}^{n_S}\sum_{p=1}^{n_P}\sum_{r=1}^{n_R}(Y_{bspr}-Y_{bsp.})^2,$$

the cross products vanishing because of the orthogonality of the design (as can straightforwardly but tediously be verified algebraically). Simplification yields

$$SST = SSB + SSS + SSP + SSR$$

Where

$$\begin{aligned}
\mathrm{SST} &= \sum_{b=1}^{n_B}\sum_{s=1}^{n_S}\sum_{p=1}^{n_P}\sum_{r=1}^{n_R}(Y_{bspr}-Y_{....})^2,\\
\mathrm{SSB} &= n_S n_P n_R \sum_{b=1}^{n_B}(Y_{b...}-Y_{....})^2,\\
\mathrm{SSS} &= n_P n_R \sum_{b=1}^{n_B}\sum_{s=1}^{n_S}(Y_{bs..}-Y_{b...})^2,\\
\mathrm{SSP} &= n_R \sum_{b=1}^{n_B}\sum_{s=1}^{n_S}\sum_{p=1}^{n_P}(Y_{bsp.}-Y_{bs..})^2,\\
\mathrm{SSR} &= \sum_{b=1}^{n_B}\sum_{s=1}^{n_S}\sum_{p=1}^{n_P}\sum_{r=1}^{n_R}(Y_{bspr}-Y_{bsp.})^2.
\end{aligned}$$

Here, the properties of nested design [21] were used to split a sum of squares at each level into two components, one of which is split into two at the next level, and so on.
In words, *SST*, the total sum of squares (of the measurements about the overall mean), is the sum of

1. *SSB*, the sum of squares of the mean values per batch about the overall mean value,

2. *SSS*, the sum of squares of the mean values per specimen per batch about *their* mean values per batch,

3. *SSP*, the sum of squares of the mean values per point per specimen per batch about *their* mean values per specimen per batch, and

4. *SSR*, the sum of squares of the replicates about their mean values per point per specimen per batch.

Now,

σ^2_B = population variance of batch means,

σ^2_S = population variance of specimen means within batches,

σ^2_P = population variance of point means within specimens,

σ^2_R = population variance of replicate measurements at points,

Assuming that these variances can be regarded as constants (in a fuller analysis this assumption would be tested).

The mean squared values are defined by

$$\begin{aligned}\mathrm{MSB} &= \mathrm{SSB}/(n_B-1),\\ \mathrm{MSS} &= \mathrm{SSS}/\{n_B(n_S-1)\},\\ \mathrm{MSP} &= \mathrm{SSP}/\{n_Bn_S(n_P-1)\},\\ \mathrm{MSR} &= \mathrm{SSR}/\{n_Bn_Sn_P(n_R-1)\}.\end{aligned}$$

$$MST = SST/\{n_b n_s n_p n_R - 1\}$$

Then estimates of $\sigma^2{}_B$, $\sigma^2{}_S$, $\sigma^2{}_P$ and $\sigma^2{}_R$ are provided by

$$\begin{aligned}\hat{\sigma}_B^2 &= (\mathrm{MSB}-\mathrm{MSS})/(n_Sn_Pn_R),\\ \hat{\sigma}_S^2 &= (\mathrm{MSS}-\mathrm{MSP})/(n_Pn_R),\\ \hat{\sigma}_P^2 &= (\mathrm{MSP}-\mathrm{MSR})/n_R,\\ \hat{\sigma}_R^2 &= \mathrm{MSR}.\end{aligned}$$

$$\hat{\sigma}^2 = MST$$

4 Post-processing

The required mass fraction for each element is taken in proportion to the number of counts corrected for the mean background count $\bar{G}$,

$$W_{bspr} = (Y_{bspr} - \bar{G})/\hat{C}.$$

$\bar{G}$ is determined from the background measurements described in Section 2, i.e., from

$$\bar{G} = \sum_{b=1}^{n_B}\sum_{s=1}^{n_S}\sum_{p=1}^{n_P}\sum_{r=1}^{n_R} G_{bspr}$$

or

$$\bar{G} = \sum_{g=1}^{m_G} G_g,$$

as appropriate.

The variances associated with the required mass fractions are related to those for the measured counts through $\hat{C}^2$ as a scaling factor. In addition, there is a component due to the variance of the mean background count $\bar{G}$ used to correct the measured counts. Since counting is assumed to be Poissonian, the variance of $\bar{G}$ is equal to $\bar{G}$ itself. Specifically, using the same symbols as those used for the variances of the unscaled quantities to denote the variances of the scaled quantities, but with an additional subscript *W* to represent mass fraction,

$$\begin{aligned}\hat{\sigma}_G^2 &= \bar{G},\\ \hat{\sigma}_{BW}^2 &= \hat{\sigma}_B^2/\hat{C}^2,\\ \hat{\sigma}_{SW}^2 &= \hat{\sigma}_S^2/\hat{C}^2,\\ \hat{\sigma}_{PW}^2 &= \hat{\sigma}_P^2/\hat{C}^2,\end{aligned}$$

$$\hat{\sigma}^2{}_W = \hat{\sigma}^2 / \hat{C}^2$$

5 Calculation procedure

There are three stages to the calculation procedure:

1. Pre-processing (problem-specific)
2. Main processing (standard ANOVA)
3. Post-processing (problem-specific).

5.1 Stage 1. Pre-processing (problem-specific)

• Input reference current I_0.

• Input certified mass fraction $\hat{W}_0$.

• Input n_B, n_S, n_P , n_R.

• For each element

– Input measured counts Y_{bspr}, $b = 1, \ldots, n_B$, $s = 1, \ldots, n_S$, $p = 1, \ldots, n_P$, $r = 1, \ldots, n_R$.

– Input corresponding background counts, either

G_{bspr}, $b = 1, \ldots, n_B$, $s = 1, \ldots, n_S$, $p = 1, \ldots, n_P$, $r = 1, \ldots, n_R$, or

G_g, $g = 1, \ldots, m_G$.

– Input measured currents I_{bspr}, $b = 1, \ldots, n_B$, $s = 1, \ldots, n_S$, $p = 1, \ldots, n_P$, $r = 1, \ldots, n_R$, corresponding to the values of Y_{bspr}.

– Correct each measurement for current drift. For $b = 1, \ldots, n_B$, $s = 1, \ldots, n_S$, $p = 1, \ldots, n_P$, $r = 1, \ldots, n_R$, replace Y_{bspr} by $Y_{bspr} \times I_0/I_{bspr}$.

5.2 Stage 2. Main processing (standard ANOVA)

• Form $Y_{bsp.}$, $b = 1, \ldots, n_B$, $s = 1, \ldots, n_S$, $p = 1, \ldots, n_P$.

• Form $Y_{bs..}$, $b = 1, \ldots, n_B$, $s = 1, \ldots, n_S$.

• Form $Y_{b...}$, $b = 1, \ldots, n_B$.

• Form $Y.....$

• Form *SST, SSB, SSS, SSP, SSR*.

Table F1: Results of the calculation of sum of squares from homogeneity study using the statistical analysis.

	Sum of squares [counts^2]	**Degrees of freedom**
SSB	21488891	2
SSS	394182750	6
SSP	656142627	927
SSR	0	936
SST	1,072E+09	1871

• Form *MSB, MSS, MSP, MSR, MST*.

Table F2: Results of the calculation of mean square from homogeneity study using the statistical analysis.

	Mean square [counts^2]
MSB	10744445
MSS	65697125
MSP	707813
MSR	0
MST	572856

• Form $\hat{\sigma}^2{}_B$, $\hat{\sigma}^2{}_S$, $\hat{\sigma}^2{}_P$, $\hat{\sigma}^2{}_R$

Table F3: Results of the calculation of variance from homogeneity study using the statistical analysis.

Symbol	Variance [counts^2]
$\hat{\sigma}^2{}_B$	-88065
$\hat{\sigma}^2{}_S$	312447
$\hat{\sigma}^2{}_P$	353907
$\hat{\sigma}^2{}_R$	0
$\hat{\sigma}^2$	572856

5.3 Stage 3. Post-processing (problem-specific)

• Form $\bar{G} = \sum_{b=1}^{n_B} \sum_{s=1}^{n_S} \sum_{p=1}^{n_P} \sum_{r=1}^{n_R} G_{bspr}/(n_B n_S n_P n_R)$ or $\bar{G} = \sum_{g=1}^{m_G} G_g.$

• Form the conversion factor $\hat{C} = (Y_{....} - \bar{G})/\hat{W}_0.$

Table F4: Results of the calculation of the conversion factor from homogeneity study using the statistical analysis.

	Symbol	Results
Background count [count]	G	2784
Certified value [g/100 g]	W	6.69
Scaling factor [count / g/100 g]	C	5814

• Form $\hat{\sigma}^2_{BW} = \hat{\sigma}^2_B/\hat{C}^2, \hat{\sigma}^2_{SW} = \hat{\sigma}^2_S/\hat{C}^2, \hat{\sigma}^2_{PW} = \hat{\sigma}^2_P/\hat{C}^2, \hat{\sigma}^2_{RW} = (\hat{\sigma}^2_R + \hat{\sigma}^2_G)/\hat{C}^2.$

Table F5: Results of the calculation of variance in [g/100 g] from homogeneity study using the statistical analysis.

Symbol	Variance [(g/100 g)^2]
$\hat{\sigma}^2{}_{BW}$	-0.0026
$\hat{\sigma}^2{}_{SW}$	0.0093
$\hat{\sigma}^2{}_{PW}$	0.0105
$\hat{\sigma}^2{}_{RW}$	0

• Form the uncertainty σ_w *from* $\hat{\sigma}^2{}_W = \hat{\sigma}^2 / \hat{C}^2$

Table F6: Results of the calculation of uncertainty from homogeneity study using the statistical analysis.

Symbol [unit]	Uncertainty
σ^2_w **[(g/100 g)^2]**	0.0170
σ_w **[g/100 g]**	0.130
σ_w **[g/kg]**	1.30

Annex G: Detailed instructions for use

The purpose of this document is to support the reader in optimising the preparation of specimens for quantitative analysis by EPMA of carbon and to suggest procedures to optimize the measurement of data collected for such analysis. The following procedures were developed and validated for the certification of IRMM-471.

1 MOUNTING

Although it can often be an advantage to mount a specimen for the analysis of carbon, the mounting medium can act as a source of contamination. It is important that the material used has excellent edge-retention properties. By using such a material the problem of leakage of carbonaceous material from any crack at the interface is minimized. Even so, it is not advised to analyse very close to the edge of the specimen. If mounted, care should be taken to ensure the CRM is flat in the mount – otherwise excess material maybe lost during repolishing.

If the CRM is not mounted it will be necessary to produce a holder capable of holding the CRM perfectly horizontal and planar, so as to allow adequate re-polishing during its lifetime. This holder is not supplied and is the responsibility of the user.

2 PREPARATION

The surface finish of the specimen to be examined should be flat, clean and dry. The specimen should be prepared in the standard metallographic manner using silicon carbide papers for grinding and diamond impregnated pads for polishing. Following a 0.25 µm diamond paste polish, the specimen should be given a final polish using 0.05 µm γ-alumina. This should be applied for a short time (30 seconds) and performed on a hard cloth. Longer polishing would produce a surface roughness and rounding of the carbide surface. Following polishing, it is important to thoroughly clean the specimen to remove any residue resulting from the preparation. This should consist of two-stage ultrasonic cleaning for approximately 5 minutes each in acetone and then ethanol. A final clean in distilled water is also recommended although it will be necessary to pay particular attention to the formation of drying stains on the specimen especially around the edge.

The specimen should not be examined in an etched condition.

If available, after the chemical cleaning the specimen surface should also be treated by a glow discharge cleaning procedure in argon. It is important to use a system with a clean high vacuum pumping stage (turbo molecular pump). An example of typical parameters used is: argon plasma pressure of 0.1 mbar and a current of 10 mA for 80 s. This cleaning procedure leads to an additional decrease of contamination due to further removal of residual hydrocarbon from the specimen surface. It is also recommended that the specimen (if ferritic) be demagnetized at this time.

3 RE-PREPARATION OF CRM

It is necessary to partially re-prepare the CRM using 0.05 µm alumina each time it is used. Care should be taken to avoid bevelling the surface. The use of gentle pressure on a hard cloth for no more than 30 seconds should minimize this risk. In addition to bevelling the CRM as a whole, care should also be taken that the individual carbides do not become rounded. The degree of re-preparation necessary will depend upon its condition. In most cases it is suggested that the ultrasonic cleaning routine described above is be adequate proceeded by wiping the surface with a cloth and ethanol. The specimen should be

examined following each re-preparation and if some surface roughness is visible, the CRM should be taken back to the diamond pads or possibly the silicon carbide papers. Although the use of a custom-built holder is strongly recommended for more drastic re-preparation (i.e. grinding and diamond polishing) it should be possible to perform the alumina polishing by hand. If a pure iron calibrant is used to determine the background value, this too should be treated as above.

4 VOLTAGE AND BEAM CURRENT

Although the optimum acceleration voltage of EPMA instrument for many types of carbide, which commonly occur in steel, is in the region of 6 kV, in practice a value of 10 to 12 kV is employed usually when measuring carbon composition. The value used in this methodology is 10 kV.

Unless spatial resolution is an issue, the beam current should be set at a high value (for analysing C in steels) typically in the range 100 to 300 nA to be consistent with good counting statistics, i.e. >10,000 counts collected in a reasonable time.

5 COUNT TIME

The longer the count time the greater the number of counts and as a consequence the smaller will be the relative uncertainty due to counting statistics. The preferred strategy will be different from instrument to instrument and depending on contamination rate during analysis. However it is recommended that at least 10000 counts should be collected to obtain an uncertainty due to counting statistics of 100 or less (i.e. 1 % relative uncertainty).

6 CONTAMINATION

The origins of the carbon that may contaminate the surface of the specimen are numerous. One source is the residual gas inside the specimen chamber. Hydrocarbons originate from the oils associated with the vacuum pumps, lubrication of the spectrometer mechanics, O-rings, cables and tubes. These can be considered as being related to the overall quality of the vacuum. Other sources include carbon on the surface of the specimen prior to insertion into the electron microscope. This may have originated from the lapping fluid used during polishing, diamond paste used in the polishing process or the residue from solvents used to clean the specimen following polishing. C-containing species on the specimen surface can never be removed completely by regular preparation or cleaning techniques, except by in-situ ion-sputtering. This is only established in UHV-analytical instruments, but not in SEMs or microprobe analysers. Many specimens, due to either their size or shape may be mounted within a medium such as Bakelite. This is an additional source of carbonaceous material, which may be distributed across the specimen during polishing If the specimen is mounted,, the risk that any small cracks at the specimen/mounting media interface may 'leak' carbonaceous residues when the specimen is placed under vacuum. This will cause severe contamination problems close to the edge of the specimen. This problem can be minimized by plating the specimen prior to mounting and grinding by a thick (>30 μm) metal layer (nickel is recommended).

7 DECONTAMINATION METHODS

In addition to basic precautions to minimize contamination such as fitting activated alumina or zeolite fore-line traps to the rotary pumps to avoid back-diffusion of oil from rotary pump to diffusion or turbo-molecular pump, it is recommended that if possible the use of the following

devices are considered (liquid nitrogen cooling, jet of gas, note that not all instruments are capable of being fitted with such devices).

A *liquid nitrogen cooling* plate placed above the specimen will minimize contamination originating from the effect of residual gases.

If a *jet of gas* is allowed to impinge on the specimen surface at the point where the electron beam hits the specimen, the rate and level of carbon contamination can be reduced considerably. Although gases such as neon do have a limited effect, the use of air or oxygen is far more effective. This is due to the cracking of the hydrocarbons on the surface of the specimen and oxidation where the beam and gas jet impinge and the products are removed by the vacuum system. It works only in connection with the electron beam.

The flow of gas through the capillary tubing should be as high as possible, while still maintaining a workable vacuum pressure in the specimen chamber.

The rate of carbon contamination and the efficiency of these decontamination devices vary considerably from instrument to instrument. The time taken to reach a plateau, after which the carbon count rate neither increases nor decreases, will also vary for a given instrument, due to the following factors**:**

Beam size. When a gas jet is used, the nature of the carbon/gas/beam interaction means that the decontamination will occur more quickly if it is limited to as small an area as possible, i.e. the carbon X-ray count rate will stabilize for a finely focussed beam more quickly than that for a defocused beam. However, the choice of beam size may be dictated by the microstructure of the specimen and the nature of the investigation. If analyses were performed using a focussed beam on a specimen with a coarse ferrite/pearlite microstructure, the results could vary from 0.3 g/kg carbon in the ferrite, to 8.3 g/kg of carbon in the pearlite, or possibly 66.9 g/kg carbon if a coarse cementite particle is analysed. Such information is not a great deal of use if the intention of the investigation is to determine the mean carbon content over an area. In such cases it is necessary to either defocus or raster the beam over an area determined by the microstructure. The beam size should be set to a value, which is as low a value as the microstructure allows. Wherever possible, the same beam size should be used on both the specimen and the CRM but this may not always be possible if the area is larger than the dimensions of the Fe_3C in the CRM. Where the investigation involves the production of a line scan across a coarse microstructure, a one-dimensional raster or line should be used, perpendicular to the direction of the actual line scan.

Voltage. The effect of the voltage of the primary beam on decontamination time was studied over the range 4 kV to 15 kV, with the result that although not as marked as the effect of beam size, a decreasing decontamination time was observed with increasing voltage. This should not be an issue if a single voltage (10 kV) is used.

An important factor accounting for the large differences in decontamination times observed between instruments is believed to be the position of the capillary tubing through which the gas jet passes, as the position of the jet relative to the beam impact site is critical. For maximum effect the jet should be as close as possible to the specimen without causing any spectrometer shadowing problems and be directed exactly at the point where the electron beam impinges on the specimen surface. On an instrument where the operator has control over the positioning of the capillary tubing it should be possible to alter the decontamination time significantly by small adjustments of the position of the capillary tubing.

In order to assess the overall cleanliness of an instrument and the efficiency of any decontamination system fitted, it is recommended that carbon data is collected on a suitably clean pure iron calibrant. This involves, for a given set of operating parameters, performing repeatedly the same carbon measurement at the same position on the specimen.

A steady increase in the carbon count rate would be indicative of a serious contamination problem. Consideration should then be given to the factors mentioned above with the aim of reversing this trend so that the instrument may be used to collect useful quantitative carbon data. However, if the count rate consistently falls it should reach a constant level after a time. The time taken to reach this plateau is defined as the decontamination time. This experiment will need to be repeated over a period of time, so the user can monitor the state of the instrument. The experiment would also need to be repeated to allow for any changes in the operating parameters such as voltage, beam size etc.

The decontamination time should be less than 10 seconds. longer decontamination times can be caused by the specimen itself, the condition of the vacuum system, the cleanliness of specimen chamber and specimen holders, the position of the gas jet or the application of the liquid N_2-system.

8 GUIDELINE FOR SPATIAL POSITION OF THE MEASUREMENT

Distance between 2 measurement points

The distances between analysis points and distance from the edge of the specimen has to be considered properly. The area around an analysis point develops a 'halo' of contamination visible as a brown or black ring surrounding a clean area. It is therefore important that one analysis point should not be so close to another that it overlaps the halo of the previous point. A reasonable distance between analysis points would be 2 micrometres when the analyses are made using a focussed beam.

However, the diameter of a focussed beam will depend upon the beam current and therefore this value is suggested as a minimum. The minimum spacing may be determined by performing line scans with increasing spot sizes and noting the distance at which subsequent values are as low as the first. Care needs to be taken that the points or areas to be analysed are chosen quickly so as to minimize any contamination prior to analysis.

Recommendation for the choice of the measurement point

Because of the risk of leakage of carbonaceous material from the specimen/mount interface, (if the specimen is mounted) the area close to the specimen edge should be avoided. If the specimen is mounted in a carbonaceous material such as Bakelite, it is probable that there will be also a greater level of carbon contamination due to the proximity of the mounting material. Even if the specimen is unmounted, the edge of the specimen may be slightly bevelled due to the effect of polishing. It is therefore advisable that again the edge of the specimen should be avoided for analysis.

Recommendation about the measurement distance to specimen surface

Analyses should not be performed closer than approximately 10 micrometres to the specimen surface (If the specimen is Ni-plated and the Ni adheres perfectly one can measure up to the surface or edge of a cross sectioned specimen.). If this is the area of interest it is recommended that the specimen is plated (nickel is suggested) to minimize these effects.

How to obtain EU publications

Our priced publications are available from EU Bookshop (http://bookshop.europa.eu),
where you can place an order with the sales agent of your choice.

The Publications Office has a worldwide network of sales agents.
You can obtain their contact details by sending a fax to (352) 29 29-42758.

European Commission
EUR 25843 EN – Joint Research Centre – Institute for Reference Materials and Measurements

Title: The certification of the mass fraction of carbon in cementite grains in a Fe-C matrix: IRMM-471

Authors: S. R. J. Saunders, T. Bacquart, J-F. Almagro, A. Braun, P. Busch, O. Couteau, D. D. Gohil, P. Karduck, G. Kerckhove, T. Linsinger, S. Richter, G. Roebben, X. Sauvage, W. G. Sloof, J-F. Thiot, M. Whitwood, T. Wirth

Luxembourg: Publications Office of the European Union

2013 – 50 pp. – 21.0 x 29.7 cm

EUR – Scientific and Technical Research series – ISSN 1831-9424 (online)

ISBN 978-92-79-28809-8 (PDF)

doi:10.2787/77197

Abstract

The report describes the production and certification of IRMM-471, a reference material certified for the carbon mass fraction of its cementite (Fe3C) grains. The Fe3C grains are dispersed within an iron pearlite matrix and present an average grain diameter between 20 µm and 50 µm. IRMM-471 has been produced and certified in order to be used as calibrant in electron probe micro-analyser (EPMA) for carbon determination in iron and steel products.

LA-NA-25843-EN-N

As the Commission's in-house science service, the Joint Research Centre's mission is to provide EU policies with independent, evidence-based scientific and technical support throughout the whole policy cycle.

Working in close cooperation with policy Directorates-General, the JRC addresses key societal challenges while stimulating innovation through developing new methods, tools and standards, and sharing its know-how with the Member States, the scientific community and international partners.

Key policy areas include: environment and climate change; energy and transport; agriculture and food security; health and consumer protection; information society and digital agenda; safety and security, including nuclear; all supported through a cross-cutting and multi-disciplinary approach.

doi:10.2787/77197

ISBN 978-92-79-28809-8

Publications Office